The Eocene-Oligocene transition at ODP Site 1263, Atlantic Ocean: decreases in nannoplankton size and abundance and correlation with benthic foraminiferal assemblages

M. Bordiga [1], J. Henderiks [1], F. Tori [2], S. Monechi [2], R. Fenero [3], and E. Thomas [4,5]

[1] Department of Earth Sciences, Uppsala University, Villavägen 16, 752 36, Uppsala (Sweden)

[2] Dipartimento di Scienze della Terra, Università di Firenze, Via la Pira 4, 50121, Florence (Italy)

[3] Departamento de Ciencias de la Tierra and Instituto Universitario de Investigación en Ciencias Ambientales de Aragón, Universidad Zaragoza, Pedro Cerbuna 12, E−50009, Zaragoza (Spain)

[4] Department of Geology and Geophysics, Yale University, New Haven, CT 06520 (USA)

[5] Department of Earth and Environmental Sciences, Wesleyan University, Middletown, CT 06459 (USA)

Correspondence to: M. Bordiga (manuela.bordiga@geo.uu.se)

Abstract

The biotic response of calcareous nannoplankton to environmental and climatic changes during the Eocene-Oligocene transition (~34.8-32.7 Ma) was investigated at high resolution at Ocean Drilling Program (ODP) Site 1263 (Walvis Ridge, South East Atlantic Ocean), and compared with a lower resolution benthic foraminiferal record. During this time interval, the global climate which had been warm during the Eocene, under high levels of atmospheric CO_2 (pCO_2), transitioned into the cooler climate of the Oligocene, with overall lower pCO_2. At Site 1263, the absolute nannofossil abundance (coccoliths per gram of sediment; N g^{-1}) and the mean coccolith size decreased distinctly across the E-O boundary (EOB; 33.89 Ma), mainly due to a sharp decline in abundance of large-sized *Reticulofenestra* and *Dictyococcites*, within ~53 kyr. Since carbonate dissolution did not vary much across the EOB, the decrease in abundance and size of nannofossils may highlight an overall decrease in their export production, which could have led to an increased ratio of organic to inorganic carbon (calcite) burial, as well as variations in the food availability for benthic foraminifers.

The benthic foraminiferal assemblage data show the global decline in abundance of rectilinear species with complex apertures in the latest Eocene (~34.5 Ma), potentially reflecting changes in the food source, thus phytoplankton, followed by transient increased abundance of species indicative of seasonal delivery of food to the sea floor (*Epistominella* spp.; ~34.04-33.54 Ma), with a short peak in overall food delivery at the EOB (buliminid taxa; ~33.9 Ma). After Oi-1 (starting at ~33.4 Ma), a high abundance of *Nuttallides umbonifera* indicates the presence of more corrosive bottom waters, possibly combined with less food arriving at the sea floor.

The most important signals in the planktonic and benthic communities, i.e. the marked decrease of large reticulofenestrids, extinctions of planktonic foraminifer species and more pronounced seasonal influx of organic matter, preceded the major expansion of the Antarctic ice sheet (Oi-1) by ~440 kyr. During Oi-1, our data show no major change in nannofossil abundance or assemblage composition occurred at Site 1263, although benthic foraminifera indicate more corrosive bottom waters following this event. Marine plankton thus showed high sensitivity to fast-changing conditions, possibly enhanced but pulsed nutrient supply, during the early onset of latest Eocene-earliest Oligocene climate change, or to a threshold in these changes (e.g. pCO_2 decline, high-latitude cooling and ocean circulation).

1 Introduction

The late Eocene-early Oligocene was marked by a ~~large~~ change in global climate and oceanic environments, reflected in significant turnovers in marine and terrestrial biota. The climate was driven from a warm "greenhouse" with high pCO_2 during the middle Eocene through a transitional period in the late Eocene to a cold "icehouse" with low pCO_2 in the earliest Oligocene (e.g. Zachos et al., 2001; DeConto and Pollard, 2003; Pearson et al., 2009; Pagani et al., 2011; Zhang et al., 2013). During this climate shift, Antarctic ice sheets first reached sea level, sea level dropped, and changes occurred in ocean chemistry and plankton communities, while the calcite compensation depth (CCD) deepened rapidly, at least in the Pacific Ocean (e.g. Zachos et al., 2001; Coxall et al., 2005; Pälike at al., 2006; Coxall and Pearson, 2007). There is ongoing debate whether the overall cooling, starting at high latitudes in the middle Eocene while the low latitudes remained persistently warm until the end of the Eocene (Pearson et al., 2007), was mainly caused by changes in oceanic gateways (opening of Drake Passage and the Tasman gateway) leading to initiation of the Antarctic Circumpolar Current as proposed by e.g. Kennett (1977), or by declining atmospheric CO_2 levels as proposed by DeConto and Pollard (2003), Barker and Thomas (2004), Katz et al. (2008) and Goldner et al. (2014), or by some combination of both (Sijp et al., 2014). Recently, it has been proposed that the glaciation itself caused further oceanic circulation changes (Goldner et al., 2014; Rugenstein et al., 2014).

The Eocene-Oligocene boundary (EOB; ~33.89 Ma, Gradstein et al., 2012) is defined by the extinction of planktonic foraminifers (specifically, the genus *Hantkenina*), and falls within this climate revolution, followed after ~450 kyr by a peak in $\delta^{18}O$, referred to as the Oi-1 event (Miller et al., 1991) which lasted for ~400 kyr and reflects intensified Antarctic glaciation (Zachos et al., 1996; Coxall et al., 2005), probably associated with cooling (e.g. Liu et al., 2009; Bohaty et al., 2012). Pearson et al. (2008), however, recorded the extinction of Hantkeninidae, thus by definition the EOB, in the plateau between the two main steps in the isotope records (i.e. within Oi-1) at Tanzania Drilling Project (TDP) Sites 11, 12 and 17. The highest occurrence of *Hantkenina* spp. may be influenced by preservation, since the taxon is sensitive to dissolution.

Recently, several high-resolution, foraminifera-based geochemical studies across the EOB, at different latitudes, have provided detailed information on the stepwise cooling (e.g. Coxall et al., 2005; Riesselman et al., 2007; Peck et al., 2010) and the dynamics of the oceanic carbon cycle across the EOB (e.g. Coxall and Pearson, 2007; Coxall and Wilson, 2011). An increase in benthic foraminiferal $\delta^{13}C$ is a major indication of changes in the carbon cycle, e.g. storage of organic matter in the lithosphere, through an increased ratio of organic to inorganic carbon (calcite) burial

due to enhanced marine export production (e.g. Diester-Haass, 1995; Zachos et al., 1996; Coxall and Wilson, 2011). There is, however, evidence that enhanced export production was not global (e.g. Griffith et al., 2010; Moore et al., 2014). The $\delta^{13}C$ shift and carbon cycle reorganization have also been related to a rapid drop in pCO_2 again linked to higher biological production and CCD deepening (Zachos and Kump, 2005).

There is a strong link between climate change and response of the marine and land biota during the late Eocene-early Oligocene. This was a time of substantial extinction and ecological reorganization in many biological groups: calcifying phytoplankton (coccolithophores; e.g. Aubry, 1992; Persico and Villa, 2004; Dunkley Jones et al., 2008; Tori, 2008; Villa et al., 2008), siliceous plankton (diatoms and radiolarians; e.g. Keller et al., 1986; Falkowski et al., 2004), planktonic and benthic foraminifers (e.g. Coccioni et al., 1988; Thomas, 1990, 1992; Thomas and Gooday, 1996; Thomas, 2007; Pearson et al., 2008; Hayward et al., 2012), large foraminifers (nummulites; e.g. Adams et al., 1986), ostracods (e.g. Benson, 1975), marine invertebrates (e.g. Dockery, 1986), and mammals (e.g. Meng and McKenna, 1998). Among the marine biota, the planktonic foraminifers experienced a synchronous extinction of five species in the Family Hantkeninidae (e.g. Coccioni et al., 1988; Coxall and Pearson, 2006). Benthic foraminiferal assemblages recorded a gradual turnover, marked by an overall decline in diversity, largely due to the decline in the relative abundance of cylindrical taxa with a complex aperture (Thomas, 2007; Hayward et al., 2012), and an increase of species which preferentially use fresh phytodetritus delivered to the seafloor in strongly seasonal pulses (e.g. Thomas, 1992; Thomas and Gooday, 1996; Pearson et al., 2008).

The calcareous nannoplankton community underwent significant changes at the EOB. Although the group did not suffer extinctions right at the boundary as the planktonic foraminifers, the structure of the assemblages underwent global reorganization. Species diversity decreased through the loss of K-selective, specialist taxa and the abundance of opportunistic species, more adapted to the new climate/environment, increased (e.g. Persico and Villa, 2004; Dunkley Jones et al., 2008; Tori, 2008). Calcareous nannoplankton, overall, flourished during the warm-oligotrophic Eocene rather than during the cold-eutrophic early Oligocene, when the siliceous diatoms become more abundant (e.g. Falkowski et al., 2004). Time series analysis (Hannisdal et al., 2012) confirmed that coccolithophores were globally more common and widespread during the Eocene, declining since the early Oligocene. On million-year time scales, atmospheric CO_2 levels influenced coccolithophore macroevolution more than related long-term changes in temperature, sea level, ocean circulation or global carbon cycling (Hannisdal et al., 2012).

In addition, the late Eocene to early Oligocene decrease in the average cell size of reticulofenestrids (presumed ancestors of modern-day alkenone producing coccolithophores) corresponds to a decline in pCO_2 (Henderiks and Pagani, 2008; Pagani et al., 2011). This macroevolutionary trend appears global and driven by the ecological decline of large reticulofenestrid species. Henderiks and Pagani (2008) hypothesized that large-celled coccolithophores were adapted to high pCO_2 and $CO_{2(aq)}$ conditions (late Eocene), whereas small-sized species became more competitive at lower pCO_2 (early Oligocene). However, this hypothesis has not yet been tested in detail.

Only few high-resolution studies have described the response of coccolithophores to environmental change across the EOB at high- (Southern Ocean; Persico and Villa, 2004; Villa et al., 2008, 2014) and low latitudes (Tanzania; Dunkley Jones et al., 2008). These studies have highlighted distinct compositional shifts and changes in species diversity at or close to the boundary. Here, we present a new high-resolution record (<10,000 kyr across the EOB) from Ocean Drilling Program (ODP) Site 1263, at mid-latitudes in the southeast Atlantic Ocean.

We report on calcareous nannofossil and foraminiferal biotic events between 34.76-32.7 Ma, to refine the shipboard biostratigraphy published in Zachos et al. (2004) and describe the ecological response to environmental change. The calcareous nannofossil assemblages reveal distinct fluctuations in total abundance and species composition, which we compare to stable isotope data (Riesselman et al., 2007; Peck et al., 2010), and to benthic foraminiferal assemblage data from the same site. For the first time, estimates of the number of nannofossils per gram of dry sediment were calculated for the Eocene-Oligocene time interval to investigate how paleo-export fluxes and food supply to the benthic community were affected. This record is also the first to investigate coccolith size variations (and related changes in mean cell size, cf. Henderiks and Pagani, 2007) across the EOB in greater detail.

2 Material and methods

2.1 ODP Site 1263

ODP Leg 208 Site 1263 (28°31.97'S and 2°46.77'E, Atlantic Ocean; Fig. 1) was drilled at a water depth of 2717 m on the southern flank of Walvis Ridge, an aseismic ridge west of the African coast. This site provides one of the most continuous sediment sequences of the early Cenozoic in the Atlantic Ocean, and was at least 1 km above the lysocline prior to the lowering of the CCD during the E-O transition (Zachos et al., 2004). Foraminifer-bearing nannofossil ooze and nannofossil ooze are the dominant lithologies in the studied interval (Zachos et al., 2004).

The Eocene-Oligocene sediments of ODP Site 1263 generally have a high carbonate content ($CaCO_3$ wt%), ranging from 88 to 96% through 84.2-100.8 mcd (Fig. 2; Riesselman et al., 2007). Only a few lower values in $CaCO_3$ (86% and 88%) have been recorded prior to the EOB, below the Oi-1 $\delta^{18}O$ excursion (Fig. 2; Riesselman et al., 2007).

A total of 190 samples was used for nannofossil analyses across the EOB in Holes 1263A and 1263B. These samples were studied in two sets, A and B. Set A includes 114 samples from 83.19 to 101.13 meters composite depth (mcd). The sampling resolution is high across the EOB (5-10 cm), and decreases above and below it: 20-90 cm between 83.19-89.6 mcd, and 20-50 cm between 97.44-101.13 mcd. An additional 76 samples were analysed in set B (83.59-105.02 mcd, sampling resolution of 10-50 cm). The two sample sets were independently analysed by different researchers, and we combine these data. For analyses on foraminiferal assemblages, 27 samples from Hole 1263A were used, from 1263A-9H-1-32-34cm (80.89 mcd) to 1263A-11H-CC (109.79 mcd).

2.2 Microfossil preparation and assemblage counts

2.2.1 Nannofossils

Sample set A was prepared by weighing 5 mg of dried sediment and diluting with 50 mL of buffered water. Then, 1.5 mL of suspension was placed on a cover slip with a high-precision pipette, and the sample was dried on a hotplate at 60°C. This technique (modified after Koch and Young, 2007) assures an even distribution of particles, and allows calculation of the absolute coccolith abundances per gram of dry sediment (N g^{-1}). Repeated sample preparation and counting revealed a coefficient of variation (CV) of 6-10%, comparable to other techniques (e.g. Bollmann et al., 1999; Geisen et al., 1999). Five samples along the studied sequence were also prepared with the filtration technique (Andruleit, 1996) and spiked with microbeads to investigate the reproducibility of absolute abundances obtained with our technique. This resulted in similar temporal trends between the techniques (mean CV=11%). The estimates of absolute abundances (N g^{-1}) allow us to better identify the real fluctuations in abundance of single species within the sediment. In contrast, the use of the relative abundances (%) could lead to loss of information and misinterpretation of the results through the closed-sum problem, as each percentage value refers to how common or rare a species is relative to other species without knowing whether a species truly increased or decreased in abundance. Sample set B was prepared with the standard smear slide technique (Bown and Young, 1998).

In both sets A and B, calcareous nannofossils were examined under crossed polarized light microscopy (LM) at 1000X magnification. Quantitative analyses were performed by counting at least 300 specimens in each slide. Additional observations were performed on the slide to detect the occurrence of rare species, especially biostratigraphical markers. All specimens were identified at species or genus level, depending on the coccolith preservation. We used *Cyclicargolithus* sp. to group the specimens with dissolved central area that can be associated to the genus *Cyclicargolithus* but not directly to the species *Cyclicargolithus floridanus* (Fig. S1 in the Supplement). Taxonomy of the calcareous nannofossils follows the reference contained in the web-site http://ina.tmsoc.org/Nannotax3 (edited by Young et al., 2014). Additional taxonomic remarks are given in the Supplement. For dataset A, the number of fields of view (FOV) observed were also noted in order to calculate absolute abundances.

Both datasets were used to provide biostratigraphical information: dataset A with a more detailed resolution across the EOB, and dataset B covering a longer interval below the EOB. For quantitative description of the nannofossil assemblage, relative abundances (%) for all the identified species were calculated for both datasets A and B.

2.2.2 Foraminifers

The 27 samples were oven-dried at 60°C, then washed over a 63 µm sieve. The complete size fraction 63 µm was studied for benthic and planktonic foraminifers. Planktonic foraminifers are abundant and benthic foraminifers common. Preservation is generally moderate, with frosty preservation of the tests. Benthic foraminifers show partial dissolution or etching, especially between 94.42 mcd and 109.79 mcd, but are generally well preserved, i.e. sufficient for determination at species level (Fenero et al., 2010).

2.3 Biotic proxies

2.3.1 Nannofossil dissolution index and cell size estimates

Sample set A was also used to characterize nannofossil dissolution across the investigated interval. A coccolith dissolution index was calculated using the ratio between entire coccoliths and fragments (cf. Beaufort et al. 2007; Blaj et al., 2009; Pea, 2010). This index is indicative of the preservation/dissolution state of the nannofossil assemblages: higher values correspond to better

preservation. Entire coccoliths and all fragments were counted until at least 300 entire coccoliths had been counted. Only pieces bigger than 3 µm were considered as fragments.

Mean coccolith and cell size estimates (volume-to-surface area ratio, V:SA; cf. Henderiks and Pagani, 2007; Henderiks, 2008) were calculated based on the relative abundance of placolith-bearing taxa (*Coccolithus*, *Cyclicargolithus*, *Dictyococcites* and *Reticulofenestra*) and the different size groups within each (3-7 µm, 7-11 µm and 11-16 µm for *Coccolithus*; 3-5 µm, 5-7 µm and 7-9 µm for all the other species).

2.3.2 Nannofossils ~~proxies~~

The distribution of coccolithophores in surface water is controlled by the availability of light, temperature, salinity and nutrient availability (e.g. Winter et al., 1994). Based on studies of modern and past paleogeographic distributions of coccolithophores, (paleo)environmental tolerances of various taxa may be determined (see Table 3 in Villa et al., 2008). However, some paleoecological labels remain unresolved or contrasting in different regions (see Table 3 in Villa et al., 2008), so our analyses aimed to circumvent such issues by not tagging certain (groups of) species a priori, but instead investigating the behaviours within total assemblages (see Section 2.4) and compare these with independent proxies (i.e. geochemical data and benthic foraminifer assemblage).

2.3.3 Foraminifera-based ~~stable isotope proxies for paleoproductivity evaluation~~

The difference between planktonic and benthic foraminiferal carbon isotope ($\Delta\delta^{13}C_{p-b}$) was proposed by Sarnthein and Winn (1990) as semi-quantitative proxy of paleoproductivity. It provides information about the surface to deep-water $\delta^{13}C$ gradient, reflecting surface paleoproductivity and stratification (e.g. Zhang et al., 2007; Bordiga et al., 2013). We calculated the $\Delta\delta^{13}C_{p-b}$ using the foraminifer data in Riesselman et al. (2007) and Peck et al. (2010).

2.3.4 Benthic foraminiferal proxies

We determined the relative abundances of benthic foraminiferal taxa, and the diversity of the assemblages was expressed as the Fisher's alpha index (Hayek and Buzas, 2010). We used changes in the relative abundances and diversity to infer changes in carbonate saturation state, oxygenation and food supply (e.g. Bremer and Lohmann, 1982; Jorissen et al., 1995, 2007; Gooday, 2003;

Thomas, 2007; Gooday and Jorissen, 2012). We interpret a high relative abundance on infaunal taxa (including the triserial buliminids) as indicative of a high, year-round food supply (Jorissen et al., 1995, 2007; Gooday, 2003). High relative abundances of phytodetritus-using taxa indicate an overall moderate, but highly seasonal or episodic flux of non-refractory particulate organic matter (e.g. Gooday, 2003; Jorissen et al., 2007), and a high relative abundance of *Nuttallides umbonifera* indicates water which are highly corrosive to $CaCO_3$ in generally low-food supply settings (Bremer and Lohmann, 1982; Gooday, 2003).

Comparisons between past and recent benthic assemblages as indicators for features of deep-sea environments need careful evaluation, because Eocene deep-sea benthic foraminiferal assemblages were structured very differently from those living today, and the ecology even of living species is not well known. For instance, in the Paleogene, taxa reflecting highly seasonal or episodic deposition of organic matter (phytodetritus) were generally absent or rare, increasing in relative abundance during the E-O transition (e.g. Thomas and Gooday, 1996; Thomas, 2007). At Walvis Ridge, these species did occur at lower abundances than in the interval studied here during the transition from early into middle Eocene (Ortiz and Thomas, 2015) and during the middle Eocene climate ~~maximum~~ (Boscolo-Galazzo et al., 2015).

In contrast, cylindrically-shaped taxa with complex apertures (called 'Extinction Group'-taxa by Hayward et al., 2012) were common (e.g. Thomas, 2007). These taxa globally declined in abundance during the increased glaciation of the earliest Oligocene and middle Miocene to become extinct during the middle Pleistocene (Hayward et al., 2012). The geographic distribution of these extinct taxa resembles that of buliminids (e.g. Hayward et al., 2012), and they were probably infaunal, as confirmed by their $\delta^{13}C$ values (Mancin et al., 2013). It is under debate what caused their Pleistocene extinction and decline in abundance across the EOB (Hayward et al., 2012; Mancin et al., 2013). Changes in the composition of phytoplankton, their food source, have been mentioned as a possible cause, as well as declining temperatures, increased oxygenation or viral infections (Hayward et al., 2012; Mancin et al., 2013).

2.4 Statistical treatment of the ~~nannoplankton~~ data

Relative species abundances are commonly observed as lognormal distributions (MacArthur, 1960). To generate suitable datasets for statistical analysis, different transformations yielding Gaussian distributions must be applied, such as log transformation (e.g. Persico and Villa, 2004; Saavedra-

Pellitero et al., 2010), centered log-ratio (e.g. Kucera and Malmgren, 1998; Buccianti and Esposito, 2004), arcsine (e.g. Auer et al., 2014), etc.

We applied two transformations to the nannofossil species percentage abundances: i) log-transformation by log(x+ 1), which amplifies the importance of less abundant species, and minimizes the dominance of few abundant species (Mix et al., 1999), and ii) centered log-ratio (clr) transformation (Aitchison, 1986; Hammer and Harper, 2006), which opens a closed data matrix and retains the true covariance structure of compositional data as well. The normal distribution of each species before and after the transformations was verified using SYSTAT 13.0 software. Datasets A and B were treated the same, but were analysed independently.

Principal component analysis (PCA) was performed on the transformed data using the statistics software PAST (PAleontological STatistic; Hammer et al., 2001). Species with an abundance <1% in all samples were not included in the PCA. The PCA (Q-mode) was performed to identify the major loading species and to evaluate the main factors affecting the changes on fossil coccolithophore assemblages.

The closed-sum problem, or constant-sum constraint, may obscure true relationships among variables as first noted by Pearson (1896) when performing statistical data analysis of compositional data. The clr transformation retains a major problem in carrying out the PCA on the covariance matrix, and the goal of keeping the most important data information with only few principal components (PCs) can fail using clr transformation in associations containing many outliers (e.g. Maronna et al., 2006) as is often the case in nannofossil assemblages. To minimize the presence of outliers we worked with abundant species and groups of nannofossils, instead of with single species.

The PAST software was used to calculate the Shannon Index, H, a diversity index taking into account the relative abundances as well as the number of taxa. High values indicate high diversity.

3 Biostratigraphy

The EOB at Site 1263 was tentatively placed between 83 and 110 mcd by the Leg 208 Shipboard Scientific Party (Zachos et al., 2004). Riesselman et al. (2007) placed Oi-1 on the basis of an increase in the benthic $\delta^{18}O$ records from ~1.5‰ (94.49 mcd, uppermost Eocene) to ~2.6‰ (93.14 mcd, lowermost Oligocene). The $\delta^{18}O$ values remained high upsection, to 88.79 mcd. Steps 1 and 2 in the $\delta^{18}O$ increase were identified ~~(Riesselman et al., 2007;~~ Peck et al., 2010), although they are not clearly defined as at Site 1218 in the Pacific Ocean (Coxall et al., 2005).

Our high-resolution sampling allowed refining the position of the EOB by locating nannofossil and planktonic foraminifer bioevents (Fig. 2; Table 1), including some nannofossil bioevents not yet reported in Zachos et al. (2004). To avoid bias, sample sets A and B were analysed by two different operators for the occurrence of nannofossil marker species (Fig. 2).

The identified bioevents are delineated as Base (B, stratigraphic lowest occurrence of a taxon), Top (T, stratigraphic highest occurrence of a taxon), and Base common (Bc, first continuous and relatively common occurrence of a taxon) according to Agnini et al. (2014), and acme beginning (AB, base of the acme of a taxon) according to Raffi et al. (2006). No correlation with magnetochrons was possible because the soft nannofossil ooze at Site 1263 does not carry a clear signal (Zachos et al., 2004).

The depths of all identified nannofossil and foraminifer datums, together with the ages assigned to the most reliable datums in Gradstein et al. (2012) are displayed in Table 1. For bioevents which are diachronous or not reported in Gradstein et al. (2012), the most recent literature was selected, considering the datums recorded at latitudes as close as possible to the studied site. The succession spans from 32.7 Ma (HO of *Isthmolithus* recurvus, Lyle et al., 2002) to 34.76 Ma (HO of *Discoaster barbadiensis*, Gradstein et al., 2012). The estimated average sedimentation rate is 9.8 m/myr, somewhat lower than the average value of 11.7 m/myr in Zachos et al. (2004). In set A, where the sample distribution is more homogeneous, the sampling resolution is ~10.000 years across the EOT (from 97.29 to 90.02 mcd).

3.1 Calcareous nannofossils

Using the absolute (N g^{-1}) and the relative (%) abundances we identified nine calcareous nannofossil datums (Fig. 2; Table 1). The studied interval spans from CP15b (pars) Zone to CP16c (pars) Zone, according to the biozonation of Okada and Bukry (1980). The bioevents include:

- B of *Sphenolithus tribulosus*, the lowermost datum identified (103.11 mcd, Table 1). The range for this bioevent (Bown and Dunkley Jones, 2006) is from Zones NP21 to NP23 (biozonation of Martini, 1971), corresponding to CP16-18 Zones. We detected this event at the top of CP15b Zone (Fig. 2), slightly below the reported range (Tori, 2008). At Site 1263, this species is not abundant and its poor preservation is commonly compromising the identification at the species level and thus possibly, its B.
- T of *Discoaster barbadiensis* and *Discoaster saipanensis*. The rosette-shaped discoasterids at the bottom of the succession are usually well preserved without overgrowth (Fig. S1 in the

Supplement). The T of *D. barbadiensis* was not identified by the Shipboard Scientific Party (Zachos et al., 2004), and we placed it one meter below the T of *D. saipanensis* (Fig. 2), identified by Zachos et al. (2004) two meters below our datum (Table 1). These two bioevents were usually considered concurrent, but high-resolution studies (Berggren et al., 1995; Lyle et al., 2002; Tori, 2008; Blaj et al., 2009) show that they are not coeval. The T of *D. saipanensis* is used to approximate the EOB and to define the CP15b/CP16a boundary.

- AB of *Clausicoccus obrutus* (>5.7 µm). The absolute abundance variations, together with the relative abundance, identify the AB at 96 mcd, ~1 m below the depth reported by the Shipboard Scientific Party (94.77 mcd; Table 1) and slightly above the observed T of *Hantkenina* spp. (Fig. 2; see the foraminifers section) – i.e. it approximates the EOB (Backman, 1987). AB of *C. obrutus* defines the base of CP16b (Okada and Bukry, 1980) as suggested by Backman (1987). This bioevent is well recognized in the Tethys Massignano GSSP and Monte Cagnero sections (Tori, 2008; Hyland et al., 2009) and also at the high latitudes Site 1090 (Marino and Flores, 2002).
- B of *Chiasmolithus altus*. The rare and discontinuous presence of *C. altus* creates some bias in the detection of its B. Moreover, *C. altus* specimens are highly affected by dissolution as their central-area is commonly completely dissolved (Fig. S1 in the Supplement). The B of *C. altus* can be placed with certainty at 89.4 mcd where a specimen with whole central crossbars meeting at 90° was observed (Fig. S1 in the Supplement). At Site 1263, the B of *C. altus*, the youngest of the genus, falls inside the lower Oligocene (Zone CP16b; Fig. 2), as also documented by de Kaenel and Villa (1996), Persico and Villa (2004), and Villa et al. (2008).
- B and Bc of *Sphenolithus akropodus*. The rare occurrence and poor preservation affect the recognition of this species, but B and Bc were identifiable (Fig. 2; Table 1). The Bc is well related with the first occurrence as identified in de Kaenel and Villa (1996), who used this bioevent to approximate the Zone NP21/22 (or CP16b/CP16c) boundary, and the T of *Coccolithus formosus*.
- T of *Coccolithus formosus*. This bioevent was easily detectable, as *C. formosus* is abundant and well preserved. Its T defines the CP16b/CP16c boundary (Fig. 2), close to the depth suggested on board ship (Table 1).
- T of *Isthmolithus recurvus*, the highest datum identified (Fig. 2). Its abundance is low, so that its distribution becomes discontinuous towards the top of the studied interval. The 83.19 mcd depth (Table 1), 3 m above that reported by the Shipboard Scientific Party (Zachos et al., 2004), is an approximation because just one sample above the last observed specimens of *I. recurvus* was analysed.

364

365 **3.2 Planktonic foraminifers**

366 At Site 1263, the primary marker species for the EOB (the genera *Cribrohantkenina* and
367 *Hantkenina*) are not well preserved, and occur as fragments of variable size, including hantkeninid
368 spines and partial specimens (several chambers). We primarily studied benthic foraminifera, so that
369 we scanned through large samples, containing thousands of specimens of planktonic foraminifera.
370 From 96.41 mcd up-section (the first higher sample being at 96.27 mcd) we did not find any
371 fragments of hantkeninid tests and/or loose spines (*Cribohantkenina* and *Hantkenina alabamensis*),
372 whereas these were consistently present in samples below that level (Fig. 2). The sample at 96.41
373 mcd contained rare spines, but no partial specimens (Fig. 2). We thus recorded the T of *H.*
374 *alabamensis*, the traditional marker for the EOB (e.g. Coccioni, 1988; Premoli-Silva and Jenkins,
375 1993; Pearson et al., 2008), at 97.91 mcd, and placed the EOB above 96.41 mcd (1263A-10H-5, 32-
376 34cm, 96.27 mcd; Table 1; Fig. 2). The benthic foraminifera at Site 1263 show some evidence of
377 reworking (Zachos et al., 2004), but this was limited to a few samples, so we consider that the
378 uppermost sample with partial tests of hantkeninids marks the uppermost Eocene. This observation
379 differs from that in Zachos et al. (2004), where only core catcher samples were studied and the
380 partial specimens in Sample 1263A-10H-CC were not observed (Table 1). Samples from Core
381 1263A-11H and sample 1263A-10H-CC (99.97-109.79) contain strongly fragmented planktonic
382 foraminifers, with non-broken specimens dominated by heavily calcified *Globigerinatheca* spp.
383 (Zachos et al., 2004).

384

385 **4 Biotic responses**

386 **4.1 Calcareous nannofossil preservation and assemblages**

387 At ODP Site 1263 no consistent increase in carbonate content above the EOB was recorded
388 (Riesselman et al., 2007), in contrast to other sites, specifically in the Pacific Ocean (e.g. Salamy
389 and Zachos, 1999; Coxall et al., 2005; Coxall and Wilson, 2011), probably because this site was
390 well above the lysocline since the late Eocene (Zachos et al., 2004). The carbonate accumulation
391 was not strongly affected by potential CCD deepening, because the $CaCO_3$ (wt%) was and
392 remained generally high (Fig. 3; Riesselman et al., 2007). The $CaCO_3$ (wt%) does not reflect the
393 total coccolith absolute abundance (Fig. 3), suggesting that also other calcifying organisms
394 (planktonic foraminifers) contributed consistently to the calcite accumulation in the sediments.

Although the site was above the lysocline during the studied time interval, the nannofossil and foraminiferal assemblages show signs of dissolution all along the sequence. Such dissolution may occur above the lysocline (e.g. Adler et al., 2001; de Villiers, 2005), leading to a reduction in species numbers and an increase of fragmentation with depth in both nannoplankton (e.g. Berger, 1973; Milliman et al., 1999; Gibbs et al., 2004) and planktonic foraminifer communities (e.g. Peterson and Prell, 1985).

At Site 1263 signs of dissolution were detected, in particular, on specimens of *Cyclicargolithus* (Fig. S1 in the Supplement) – one of the least resistant species (Blaj et al., 2009), but also on more robust species like *Dictyococcites bisectus* (Fig. S1 in the Supplement). The absence of specimens <3 µm is indicative of dissolution, but does not prevent the identification of the main features in the assemblage. The coccolith dissolution index does not show large changes at the EOB, but during and after the Oi-1 nannofossil dissolution slightly intensified (Fig. 3). The correlation between the dissolution index and total coccolith abundance is positive and stronger in the upper interval of the studied sequence, but not significant across the EOB. In fact, from 90.5 mcd upward the correlation value, r, is 0.59 (p-value = 0.002), instead for the entire interval r = 0.32 (p-value = 0). This confirms that the total coccolith abundance and the nannofossil assemblage features are preserved in the fossil record, at least across the EOB, although nannofossil dissolution may be intense. ~~From~~ 90.5 mcd ~~u~~p-section, dissolution more strongly affected the assemblages.

The total absolute coccolith abundance records a marked decrease across the EOB: within 60 cm (from 96.39 to 95.79 mcd) the abundance rapidly drops by 45%, mainly driven by the loss of large-sized species, in particular of *D. bisectus* (Fig. 3).

Nannofossil diversity, based on the H index, does not record significant variations at the EOB. A more distinct step-wise decrease is recorded at 90 mcd (grey bar in Fig. 3), which could be explained by the increased dissolution in this interval, and by a community structure with fewer dominant species. Actually, in this interval *Cyclicargolithus* became more dominant in the assemblage, while large *Reticulofenestra* decreased in abundance significantly (Fig. 3). The calcareous nannofossil assemblage variations recorded in sample sets A and B are comparable despite the different sampling resolution (Figs. S2 and S3 in the Supplement).

The absolute abundances of all the large-sized species decreased markedly across the EOB (Fig. 3), including the species *D. bisectus*, *Dictyococcites stavensis*, *Reticulofenestra umbilicus*, *Reticulofenestra samodurovii*, *Reticulofenestra hillae*, *Reticulofenestra* sp.1 (see taxonomical remarks in the Supplement), and *Reticulofenestra daviesii*. Among these, *D. bisectus* and *D. stavensis* constitute a significant part (up to 28%) of the assemblage.

The small-medium *Cyclicargolithus* sp. and *C. floridanus* are the most abundant species (up to 50%), and the 5-7 µm size group is dominant. This group increases slightly from the bottom upwards, but at the EOB only a slight decrease in absolute abundance is recorded. Also, *C. pelagicus* is one of the most important components of the nannofossil assemblage, at a maximum abundance of 27% (Fig. 3). This species increases its absolute abundance between 96.79-92.6 mcd, i.e. across and above the EOB, and then it decreases from 88 mcd upwards. *Sphenolithus* spp. also does not show marked variation at the EOB, even if this group is not very abundant. This lack of any species that increase in abundance above the EOB at Site 1263 suggests that the loss in large reticulofenestrids was not compensated for by other taxa, leading to a sustained decrease in total coccolith abundance (and export production) since the EOB.

Another component of the assemblage, *Lanternithus minutus,* is generally not abundant, but peaks between 89.6 and 87.12 mcd. *Zygrablithus bijugatus* and *Discoaster* spp. both decreased in abundance before the EOB and, thereafter, never reached abundances as high as in the late Eocene.

4.1.1 Principal component analysis

The PCAs performed on datasets A and B give fairly comparable results, either using the log- or clr-transformation. For dataset A, the Pearson correlation value (r) between the components from the two transformations is 0.90 (p-value=0), confirming that the primary signals in the assemblage are revealed by the multivariate statistical analysis, as long as the normal distribution of the species is maintained. We also compared the PCA results with or without the presence of the marker species, because stratigraphically-controlled species are not distributed along the entire succession, thus affect PCA outcomes (e.g. Persico and Villa, 2004; Maiorano et al., 2013). Nonetheless, the results obtained with and without the marker species still provide similar trends because in the studied interval the marker species are not very abundant (Fig. 4; Table S1 in the Supplement).

In the following discussion, we will focus on the PCA results and the loading species using the log-transformation for datasets A and B (Fig. 4; Tables S1 and S2 in the Supplement). The only two significant principal components explain 50% of the total variance in dataset A, and respectively account for 36% and 14%. For dataset B the two components explain 35% (26% and 11% respectively).

Principal component 1 (PC1) of dataset A shows positive values below 96 mcd. A pronounced decrease occurs at the EOB, and from 96 mcd upwards the PC1 maintains mainly negative values (Fig. 4a). PC1 is negatively loaded by *C. obrutus*, *C. floridanus* small and medium size, and

positively by *D. stavensis*, *D. bisectus*, *R. daviesii*, and *R. umbilicus* (Fig. 4a; Table S1 in the Supplement). The loadings of the other species are too low to be significant. The PC1 of dataset B does not record the same marked drop at the boundary, but rather a gradual decrease all along the sequence (Fig. 4a). Although the main loading species are the same for both datasets (i.e. *C. obrutus*, *Cyclicargolithus* versus *D. bisectus* and *R. umbilicus*) some differences can be identified (Table S2 in the Supplement). In particular, the influence of *Cyclicargolithus* size groups on PC1 cannot be detected in dataset B because the size subdivision was not included in the count. As the distribution of large vs small-medium sized species on the PCA seems to be important for both datasets and *Cyclicargolithus* is one of the most abundant species, it is possible that the lack of a detailed size grouping within this genus in dataset B could lead to the difference in the PC1 curves at the EOB. The higher abundances of *Discoaster* and *R. umbilicus* from the bottom up to 102 mcd in dataset B could also explain some differences in the loading species between the two datasets (Tables S1 and S2, and Fig. S3 in the Supplement).

Principal component 2 (PC2) of dataset A also records an abrupt variation across the EOB: the negative values at the bottom of the succession turn toward positive values above the boundary and remain positive up to 89.95 mcd. From 89 mcd upwards, PC2 displays mainly negative values again, except for a peak between 85.68-86.42 mcd (Fig. 4b). The most meaningful species loading on PC2 is *L. minutus* (negative loading). The PC2 is also loaded negatively by *D. stavensis* and *C. floridanus* (5-7 µm), and positively by *C. pelagicus* (3-7 µm and 7-11 µm), *I. recurvus* and *Sphenolithus* spp. (Fig. 4b; Table S1 in the Supplement). The PC2 for dataset B shows a similar trend as dataset A from 98 mcd upward (Fig. 4b), but it distinctly differs in the lower part of the succession. Again, the PC2 is resolved by the same main loading species *L. minutus* versus *C. pelagicus* (but note that the relative direction (positive or negative) of the loadings is swapped between dataset A and B; Tables S1 and S2 in the Supplement). In particular, *L. minutus* has very strong loadings in both datasets. In dataset B *L. minutus* has its maximum abundance in the upper Eocene interval that was not sampled in dataset A (Fig. S3 in the Supplement), likely driving the differences between the two PC2 curves below the EOB (Fig. 4b). The distribution of *L. minutus* becomes more comparable between the datasets above 100 mcd, reaching a peak between 89.6 and 87.12 mcd although not as high as during the upper Eocene (Figs. S2 and S3 in the Supplement).

In the following discussion, we used the PCA results for dataset A (without the markers) only, because of its more even sample distribution and direct comparison to the other available nannofossil proxies, i.e. dissolution index, coccolith size distribution and absolute abundance.

4.2 Mean coccolithophore cell size variations

The PC1 curve is mirrored (r=0.81; *p*-value=0) by mean cell size estimates (V:SA ratio) of all placolith-bearing coccolithophores within the assemblages (Fig. 5). Fluctuations in mean size are mainly driven by the relative abundance of the different placolith-bearing taxa and their respective size groups, rather than intra-specific size variations. The mean V:SA ratios were higher (large cells were more abundant) during the late Eocene, and decreased by 8% across the EOB, within 60 cm above (from 96.39 to 95.79 mcd), or ~53 kyr.

Our coccolith dissolution index confirms that preferential dissolution of small species did not bias the V:SA results, as intervals of increased dissolution did not generally correspond to large V:SA (r = -0.12). The only exception is the top, 90-90.3 mcd, interval where a high dissolution peak corresponds to an increase in mean size.

4.3 Benthic foraminifer assemblage

The low resolution data on benthic foraminifera show that the diversity of the assemblages (see Fisher's alpha index curve; Fig. 6) started to decline in the late Eocene (~34.5 Ma; 102.79 mcd), reached its lowest values just below the EOB, then slowly recovered, but never to its Eocene values (Fenero et al., 2010). The decline in diversity was due in part to a decline in relative abundance of rectilinear species with complex apertures ('extinction group' species). Such a decline is observed globally at the end of the Eocene (Thomas, 2007; Hayward et al., 2012). The declining diversity was also due to a transient increase in abundance of species indicative of seasonal delivery of food to the sea floor (phytodetritus species, mainly *Epistominella* spp.; ~34.04-33.51 Ma; 97.91-91.91 mcd), with a short peak in overall, year-round food delivery at the E/O boundary (buliminid taxa; ~33.9 Ma; 96.41-96.27 mcd). After Oi-1 (starting at ~33.4 Ma; 90.41 mcd), the abundance of *N. umbonifera* increased. Due to evidence for dissolution, benthic foraminiferal accumulation rates can not be used to estimate food supply quantitatively and reliably.

5 Discussion

5.1 Nannoplankton abundance and cell size decrease at the EOB

The distinct variation in nannoplankton abundance and average coccolith size across the EOB at Site 1263 cannot be explained by dissolution or a change in species diversity, but is mainly linked changes in community structure (Fig. 3). The drop in total nannofossil abundance (Fig. 3) and mean

cell size (Fig. 5) is mainly driven by the decrease in abundance of large *Reticulofenestra* and *Dictyococcites* across the EOB. The mean V:SA estimates for all ancient alkenone producers combined (i.e. *Cyclicargolithus*, *Reticulofenestra* and *Dictyococcites*; Plancq et al., 2012) tightly overlap (Fig. 5) with biometric data of the same group in the Equatorial Atlantic (Ceara Rise, ODP Sites 925 and 929; Pagani et al., 2011), while the mean size estimates for combined *Reticulofenestra* and *Dictyococcites* coincide with mean values measured at ODP Site 1090 in the Subantarctic Atlantic, where *Cyclicargolithus* spp. were not present and assemblages are likely severely affected by dissolution (Pea, 2010; Pagani et al., 2011).

The assemblage records illustrate the mid-latitude location of Site 1263, hosting both "subantarctic" and "equatorial" taxa. A striking correspondence with the mean V:SA of ancient alkenone producers at Site 1263 and Sites 929 and 925 (Fig. 5) would suggest more affinity with tropical assemblages than with high-latitude ones, south of the Subtropical Convergence (STF). The abundance patterns of the larger reticulofenestrids, however, are strikingly similar to those at Southern Ocean sites (Persico and Villa, 2004; Villa et al., 2008). The mid-latitudinal Site 1263 thus probably records paleobiogeographic patterns in the nannofossil assemblage intermediate between those in equatorial-tropical and subantarctic regions.

The coccolith size-shift and the decreased abundance of large reticulofenestrids across the EOB may be related to different bio-limiting factors. Under growth-limiting environmental conditions, phytoplankton (coccolithophores) with small cell volume-to-surface area ratios may outcompete larger cells due to lower resource requirements (lower C, P and N cell quota) and generally higher growth rates (e.g. Daniels et al., 2014). A change in overall nutrient regime, such as in coastal upwelling vs. oligotrophic, stratified gyre systems, may also cause a shift in opportunistic vs. specialist taxa (e.g. Falkowski et al., 2004; Dunkley Jones et al., 2008; Henderiks et al., 2012). The 16-37% absolute abundance declines of the reticulofenestrid species *D. bisectus*, *R. umbilicus*, *R. hillae* and *R. daviesii* (Fig. 3), are strong indications that these large-celled coccolithophores were at a competitive disadvantage already during or shortly after the EOB. Earlier biometric studies of reticulofenestrid coccoliths point to a similar scenario (Fig. 5), postulating that the macroevolutionary size decrease reflects the long-term decline in pCO_2 (Henderiks and Pagani, 2008; Pagani et al. 2011). High CO_2 availability during the late Eocene could have supported high diffusive CO_2-uptake rates and photosynthesis even in the largest cells, assuming that ancient coccolithophores had no or inefficient CO_2-concentrating mechanism, similar to modern species today (Rost et al., 2003), and due to the fact that R~~ubisco's~~ specificity for CO_2 increases at higher CO_2 levels (Giordano et al., 2005).

Available paleo-pCO_2 proxy reconstructions from Equatorial regions (Pearson et al., 2009; Pagani et al., 2011; Zhang et al., 2013) indicate a transient decrease in pCO_2 across the studied interval rather than a distinct drop in pCO_2 at the EOB, which would be suggested by our high-resolution assemblage (PC1) and mean V:SA time series (Fig. 5). Nevertheless, the paleo-pCO_2 proxy data are at much lower resolution, based on a range of geochemical proxies and assumptions (Pearson et al., 2009; Pagani et al., 2011; Zhang et al., 2013), and may therefore not record the drop in pCO_2 as accurately as our comparative analysis would require. The range of estimated pCO_2 values is fairly wide: mean values are 940 ppmv below the EOB (standard deviation range 740-1260 ppmv) and 780 ppmv above the boundary (s.d. range 530-1230 ppmv) (Fig. 5).

Possibly, during the EOB a threshold level in pCO_2 was reached, below which large reticulofenestrids became limited in their diffusive CO_2-uptake, or other, fast-changing (a)biotic environmental factors limited the ecological success of the same group. Between biotic and abiotic factors, the latter (i.e. nutrient supply, temperature, salinity, etc.) are deemed to be dominant (Benton, 2009), and may have led to a more successful adaptation of the smaller taxa at the expenses of the large ones (see discussion below, Section 5.2).

This would not exclude a transient, long-term pCO_2 forcing on coccolithophore evolution (Hannisdal et al., 2012). Interestingly, the decline of large *R. umbilicus* occurred earlier at Site 1263 (across the EOB ~33.89 Ma) than at higher latitudes in the Southern Ocean (just above the EOB: ~33.3 Ma, Persico and Villa, 2004; ~33.5 Ma, Villa et al., 2008). A similar pattern is documented in the timing of its subsequent extinction, occurring earlier at low- and mid-latitudes (32.02 Ma; Gradstein et al., 2012) and later in high latitudes (31.35 Ma; Gradstein et al., 2012). Henderiks and Pagani (2008) suggested that the generally higher content of CO_2 in polar waters may have sustained *R. umbilicus* populations after it had long disappeared from the tropics.

5.2 Paleoproductivity at Site 1263: nannoplankton and benthic foraminifer signals

At Site 1263, no other phytoplankton than calcareous nannoplankton was detected, and diatoms were also absent in coeval sediments at near-by Deep Sea Drilling Program (DSDP) Walvis Ridge Sites 525-529 (Moore et al., 1984). Therefore, our inferences of paleo-primary productivity and export production are based on the nannoplankton and benthic foraminifer assemblages.

PC2 of the calcareous nannoplankton analysis could be correlated with paleoproductivity and total water column stratification. The strongest negative loading on PC2 is the holococcolith *L. minutus* (Fig. 4b; Table S1 in the Supplement). In modern phytoplankton, the holococcolith-bearing life

stages proliferate under oligotrophic conditions (e.g. Winter et al., 1994). Moreover, holococcoliths such as *L. minutus* and *Z. bijugatus* are quite robust (Dunkley Jones et al., 2008), so that dissolution is unlikely to affect their distribution which may be mainly linked to low nutrient availability.

The positive loadings on PC2 are the species *C. pelagicus*, *I. recurvus* and *Sphenolithus* spp. A high abundance of *C. pelagicus* has often been considered as indicative for warm-to-temperate temperatures (e.g. Wei and Wise, 1990; Persico and Villa, 2004; Villa et al., 2008). In the modern oceans, *C. pelagicus* seems to be restricted to cool-water, high-nutrient conditions (e.g. Cachao and Moita, 2000; Boeckel et al., 2006), but during the Paleogene it was cosmopolitan (Haq and Lohmann, 1976).

We compared PC2 with the proxy for paleoproductivity $\Delta\delta^{13}C_{P\text{-}B}$ (Fig. 6), with lower values corresponding to lower productivity or higher stratification. The $\Delta\delta^{13}C_{P\text{-}B}$ data are not available for the interval below 96 mcd (upper Eocene), but lower paleoproductivity in general corresponds to negative loadings on PC2, and vice versa. The correlation coefficient between the two curves is 0.33 (*p*-value =0.05), i.e. a significant but not a very strong correlation, possibly due to the lower number of stable isotope data points. We infer that PC2 probably reflects lower productivity during the latest Eocene, and both PC2 and $\Delta\delta^{13}C_{P\text{-}B}$ curves show a higher productivity signal at the onset of Oi-1 (Fig. 6). In particular, PC2 records a longer interval of higher productivity above the EOB, and an initial decrease before the highest peak in $\delta^{18}O$ (at~93 mcd; ~33.6 Ma), as recorded also by $\Delta\delta^{13}C_{P\text{-}B}$. Paleoproductivity subsequently remained lower from the end of Oi-1 upward. The PC2 and $\Delta\delta^{13}C_{P\text{-}B}$ curves differ from 90.5 mcd upward, possibly related to increased nannofossil dissolution. The increase of dissolution is confirmed by the increased abundance of the benthic foraminifer species *N. umbonifera* (Fig. 6), indicative of more corrosive bottom waters or possibly a lower food supply. This is thus in agreement with the intensified dissolution interval recorded by the coccolith dissolution index (compare Figs. 3 and 6).

The benthic foraminifer assemblage confirms the interpretation of the PC2, adding information on the nature of the nutrient supply (Fig. 6). The increase across the EOB of the phytodetritus species indicates an increase in seasonal delivery of food to the seafloor, correlated to the interval with positive scores in PC2 (Fig. 6), though interrupted by a short interval of increased productivity across the EOB (as showed by the peak in the buliminid species curve at 96.27 mcd; Fig. 6). After the Oi-1, the high abundance of *N. umbonifera* and the decrease of phytodetritus and buliminid species are indicative of more corrosive bottom waters, possibly combined with less food arriving at the sea floor and/or a less pronounced seasonality (Fig. 6).

The variations in nutrient supply, as reflected in both nannofossil and benthic foraminifer assemblages, could possibly have driven the mean coccolith size decrease across the EOB. In fact, the transient higher availability of nutrients at the onset of Oi-1, may have made it possibly for small opportunistic species above the EOB to outcompete large specialist species. The decrease of mean cell size (less biomass per individual) and, also, of total nannofossil abundance could have led to less available organic matter and, thus, less food for the benthic foraminifers, and smaller nannoplankton could have caused a decrease in delivery of organic matter to the seafloor (and/or higher remineralization).

Possibly, major instability of the water column during the onset of Oi-1 favoured seasonal or episodic upwelling, thus primary productivity in this area, but an increase in productivity at the Oi-1 onset is not reflected in the absolute coccolith abundance (Fig. 3). After the major peak in $\delta^{18}O$ (Oi-1) a more stable system, related also to the onset of North Atlantic Deep Water (NADW) production in the early Oligocene (Via and Thomas, 2006), may have allowed the proliferation of more oligotrophic taxa, including holococcoliths, and the establishment of more oligotrophic environmental conditions (Fig. 6).

Previous studies have documented an increase in primary productivity during the late Eocene-early Oligocene, in particular in the Southern Ocean (e.g. Salamy and Zachos, 1999; Persico and Villa, 2004; Schumacher and Lazarus, 2004; Anderson and Delaney, 2005). At tropical latitudes, both transient increases (equatorial Atlantic; Diester-Haass and Zachos, 2003) and decreases (e.g. Griffith et al., 2010; Moore et al., 2014) in paleoproductivity have been recorded during the early Oligocene, with a sharp drop in the export productivity in the early Oligocene at ~33.7 Ma (Moore et al., 2014), similar to what we observed in the southeastern Atlantic. Schumacher and Lazarus (2004) did not record a significant shift of paleoproductivity at the EOB in equatorial oceans, but noted a decrease in the early Oligocene (after 31 Ma). An increase in seasonality at the EOB, similar to the one we recorded at mid-latitudinal Site 1263, was documented at Site 689 in Southern Ocean (Schumacher and Lazarus, 2004), and seasonality increased just before Oi-1 in the northern high latitudes as well (Eldrett et al., 2009).

5.3 Timing and possible causes of the biotic response at the EOB

Marine faunal and floral species extinctions and community changes were coeval with the climatic deterioration during the late Eocene-early Oligocene (e.g. Adams et al., 1986; Coccioni, 1988; Berggren and Pearson, 2005; Dunkley Jones et al., 2008; Pearson et al., 2008; Tori, 2008; Villa et

al., 2008, 2014). At ODP Site 1263, we also see close correspondence between marked changes in the nannoplankton assemblages (i.e. nannofossil abundance and coccolith size decrease) and the extinction of the hantkeninid planktic foraminifers. Both events occurred at the EOB, pre-dating the onset of Oi-1, i.e. the first major ice sheet expansion on Antarctica. Extinction events are usually rapid (10-100 kyr; Gibbs et al., 2005; Raffi et al., 2006). The nannoplankton did not suffer significant extinctions at the same boundary, but the change in the community was relatively fast, taking place within ~53 kyr

The timing of the main shifts in the planktonic community was relatively early during the transient climate change across the EOB, and pre-dated significant cooling and increase in Antarctic ice sheet volume by about 440 kyrs (i.e. Oi-1). Therefore, fossil planktonic assemblages are fundamentally important and accurate tools to investigate early impacts or crossing of threshold levels during climate change on biotic systems.

Benthic foraminiferal changes at Site 1263 likewise started before the EOB (Thomas, 1990, 2007), and the faunal turnover persisted into the early Oligocene. The benthic faunas in general show a decline in rectilinear species, possibly linked to the decline in nannoplankton species which may have been used by the rectilinear benthics (as e.g. hypothesized by Hayward et al., 2012, Mancin et al., 2013). The increase in phytodetritus-using species was possibly linked to more episodic upwelling and thus productivity, and potentially blooming of more opportunistic nannoplankton species. Unfortunately, the lower resolution of the benthic foraminifer data compared to the nannofossil data does not allow to unravel the exact timing of the benthic fauna response across the EOB.

At Site 1263 and in Southern Ocean records (Persico and Villa, 2004; Villa et al., 2008) the large reticulofenestrids declined in abundance rapidly at the EOB. Persico and Villa (2004) and Villa et al. (2008, 2014) inferred a strong influence of SST cooling on coccolithophores, and the drop in SST across the EOB at high-latitudes is also confirmed by a decrease of 5°C in $U^{K'}_{37}$-based SST (Liu et al., 2009). In contrast, at Site 1263 planktonic foraminifer Mg/Ca data record no significant change in SST at that time (Peck et al., 2010; Fig. 5), as at ODP Sites 925 and 929 (tropical western Atlantic) where $U^{K'}_{37}$-based SSTs also show no relevant cooling (Liu et al., 2009; Fig. 5). Fairly stable SSTs were also documented in the tropics using Mg/Ca-based SST reconstructions (Lear et al., 2008). The temperatures at mid-latitudinal Site 1263 thus may have been stable, like those in the tropics, rather than cooling, as inferred for high latitudes in the Southern Ocean (e.g. Persico and Villa, 2004; Villa et al., 2008; Liu et al., 2009; Villa et al., 2014).

If this is true, SST may not have been the main environmental factor affecting the nannoplankton assemblages at Site 1263 across the EOB. Andruleit et al. (2003) documented that for modern coccolithophores in tropical-subtropical regions temperature changes may be of less importance, but the lower temperature at high latitudes can approach the vital limits for coccolithophores (Baumann et al., 1997), and become important as a bio-limiting factor.

Changes in the phytoplankton community could be related to a global influence of declining pCO_2. Unfortunately the estimates available from alkenone- and boron isotopes lack the resolution to unravel the variation at the EOB (Fig. 5), but leave open the possibility that falling pCO_2 below a certain threshold-level could have played a role in driving the reorganization in the nannoplankton community. Alternatively, our combined biotic and geochemical proxy data (i.e. nannofossil and benthic foraminifer assemblages, and $\Delta\delta^{13}C_{P\text{-}B}$) suggest an increase in nutrient and food supply just after the EOB (Fig. 6), which would have favored opportunistic taxa over low-nutrient selected, specialist species. We conclude that the large reticulofenestrids were clearly at an ecological disadvantage, either due to changes in nutrient supply and/or pCO_2, whereas *Cyclicargolithus* and *Coccolithus* remained unaffected, or slightly increased in absolute abundance. Most large reticulofenestrids (except *R. hillae* and *Reticulofenestra* sp.1) never recovered to pre-EOB abundances, despite a return to more stratified conditions after the Oi-1 event. Increased dissolution after the Oi-1 event unlikely explains the loss of large, heavily calcified taxa, but may also have led to enhanced remineralization of organic matter and less food supply to the benthic communities.

A regional increase in nutrients after the EOB was also postulated to have occurred at low latitudes, based on a decrease in nannofossil species diversity at Tanzanian sites (Dunkley Jones et al., 2008). At Site 1263, no marked change in diversity was recorded at the EOB (Fig. 3). The diversity and species richness of fossil assemblages, however, are strongly affected by dissolution, or by reworking and taxonomic errors (Lazarus, 2011; Lloyd et al., 2012). The Tanzanian sites indeed reveal remarkable and pristine marine microfossil preservation (Dunkley-Jones et al., 2008; Pearson et al., 2008), rarely matched by other Eocene-Oligocene deep-sea records.

There appears to be a latitudinal gradient in the timing of nannofossil abundance decreases. The abundance decreases were first detected in the Southern Ocean (late Eocene; Persico and Villa, 2004), then at mid-latitude (at the EOB; this study), and finally at the equator (after the Oi-1; Dunkley Jones et al., 2008). So that may suggest a direct temperature effect on nannoplankton abundance since the cooling started and was most pronounced at high latitudes, or indirect high-latitude cooling impacts on global nutrient regimes and ocean circulation. Since regional dissolution bias may also affect the comparison of absolute coccolith abundance, additional studies on well-

preserved material will be necessary to confirm the timing and character of the response at different latitudes and in different ocean basins. Nevertheless, a meridional gradient in biotic response is expected, given the different environmental sensitivities and biogeographic ranges of different phytoplankton species (e.g. Wei and Wise, 1990; Monechi et al., 2000; Persico and Villa, 2004; Villa et al., 2008), and the diachroneity of the onset of cooling (Pearson et al., 2008).

6 Conclusions

High-resolution analyses of the calcareous nannofossil and foraminifer assemblages refine the biostratigraphy at ODP Site 1263 (Walvis Ridge), and demonstrate distinct assemblage and abundance changes in marine biota at the Eocene-Oligocene ~~boundary.~~ The biotic response of calcareous nannoplankton was very rapid (~53 kyr), ~~similar~~ to the hantkenid extinction event, and pre-dated the Oi-1 event by 440 kyr.

The ecological success of the small-sized coccolithophore species versus the drastic decrease of large ones, and the overall decrease of nannoplankton productivity across the EOB may have affected the benthic foraminiferal community (e.g. decrease in rectilinear species due to changes in nannoplankton floras), with increased seasonality driving the transient increased abundance of phytodetritus-using species. After Oi-1, both nannoplankton and benthic records are affected by intensified dissolution and corrosivity of bottom waters.

We conclude that the planktonic community reacted to some fast-changing environmental conditions, possibly seasonally increased nutrient supply to the photic zone, global cooling or lowered CO_2-availability, or the crossing of a threshold-level along the longer-term (transient) climate and environmental changes suggested by available proxy data, such as the pCO_2 decline during the late Eocene-early Oligocene.

Supplement data file contains: Tables S1 and S2 (loading species for datasets A and B); taxonomic remarks; Fig. S1 (plate of main species); Figs. S2 and S3 (plotted curves of all the distinguished species in datasets A and B).

Acknowledgments

The authors are grateful to the International Ocean Discovery Program (IODP) core repository in Bremen for providing samples for this research. The ODP (now IODP) was sponsored by the US National Science Foundation and participating countries under management of the Joint Oceanographic Institutions (JOI), Inc. The project was financially supported by the Swedish Research Council (VR grant 2011-4866 to J.H.), and by MIUR-PRIN grant 2010X3PP8J 005 (to S.M.). We thank the Geological Society of America and the Leverhulme Foundation (UK) for research support. We are grateful to Davide Persico and Nicholas Campione for discussions on the statistical approach.

References

Adams, C. G., Butterlin, J., and Samanta, B. K.: Larger foraminifera and events at the Eocene-Oligocene boundary in the Indo–West Pacific region, in*:* Terminal Eocene Events, edited by: Pomerol, C. and Premoli Silva, I., Elsevier, Amsterdam, 237–252, 1986.

Adler, M., Hensen, C., Wenzhöfer, F., Pfeifer, K., and Schulz, H. D.: Modelling of calcite dissolution by oxic respiration in supralysoclinal deep-sea sediments, Mar. Geol., 177, 167–189, 2001.

Agnini, C., Fornaciari, E., Raffi, I., Catanzariti, R., Pälike, H., Backman, J., and Rio, D.: Biozonation and biochronology of Paleogene calcareous nannofossils from low and middle latitudes, Newsletters on Stratigraphy, 47, 131–181, 2014.

Aitchison, J.: The statistical analysis of compositional data. Chapman and Hall, London, 416 pp., 1986.

Anderson, L. D. and Delaney, L. M.: Middle Eocene to early Oligocene paleoceanography from the Agulhas Ridge, Southern Ocean (Ocean Drilling Program Leg 177, Site 1090), Paleoceanography, 20, PA1013, doi:10.1029/2004PA001043, 2005.

Andruleit, H.: A filtration technique for quantitative studies of coccoliths, Micropaleontology, 42, 403–406, 1996.

Andruleit, H., Stäger, S., Rogalla, U., and Čepek, P.: Living coccolithophores in the northern Arabian Sea: ecological tolerances and environmental control. Mar. Micropaleontol., 49, 157–181, 2003.

Aubry, M.-P.: Late Paleogene calcareous nannoplankton evolution; a tale of climatic deterioration, in: Eocene-Oligocene Climatic and Biotic Evolution, edited by: Prothero, D. R. and Berggren, W. A., Princeton University Press, 272–309, 1992.

Auer, G., Piller, W. E., and Harzhauser, M.: High-resolution calcareous nannoplankton palaeoecology as a proxy for small-scale environmental changes in the Early Miocene, Mar. Micropaleontol., 111, 53–65, 2014.

Backman, J.: Quantitative calcareous nannofossil biochronology of middle Eocene through early Oligocene sediment from DSDP Sites 522 and 523, Abhandlungen der Geologischen Bundesanstalt, Vienna, 39, 21–31, 1987.

Barker, P. F. and Thomas, E.: Origin, signature and palaeoclimatic influence of the Antarctic Circumpolar Current, Earth Science Reviews, 66, 143–162, 2004.

Baumann, K.-H., Andruleit, H., Schröder-Ritzrau, A., and Samtleben, C.: Spatial and temporal dynamics of coccolithophore communities during non-production phases in the Norwegian-Greenland Sea, in: Contributions to the Micropaleontology and Paleoceanography of the Northern North Atlantic, edited by: Hass, H. C. and Kaminski, M. A., Grzybowski Foundation Special Publication, 5, 227–243, 1997.

Beaufort, L., Probert, I., and Buchet, N.: Effects of acidification and primary production on coccolith weight: Implications for carbonate transfer from the surface to the deep ocean, Geochem. Geophy. Geosy., 8, 1–18, 2007.

Benson, R. H.: The origin of the psychrosphere as recorded in changes of deep-sea ostracode assemblages, Lethaia, 8, 69–83, 1975.

Benton, M. J.: The Red Queen and the Court Jester: species diversity and the role of biotic and abiotic factors through time, Science, 323, 728–732, 2009.

Berger, W. H.: Deep-sea carbonates: evidence for a coccolith lysocline, Deep-Sea Research and Oceanographic Abstracts, 20, 917–921, 1973.

Berggren, W. A. and Pearson, P. N.: A revised tropical to subtropical Paleogene planktonic foraminifera zonation, J. Foramin. Res., 35, 279–298, 2005.

Berggren, W. A., Kent, D. V., Swisher, C. C., and Aubry, M.-P. A revised Cenozoic geochronology and chronostratigraphy, in: Geochronology, time scales and global stratigraphic correlation, SEPM Spec. Publ., 54, 129–212, 1995.

Blaj, T., Backman, J., and Raffi, I.: Late Eocene to Oligocene preservation history and biochronology of calcareous nannofossils from paleo-equatorial Pacific Ocean sediments, Riv. Ital. Paleontol. S., 115, 67–85, 2009.

Boeckel, B., Baumann, K.-H., Henrich, R., and Kinkel, H.: Coccolith distribution patterns in South Atlantic and Southern Ocean surface sediments in relation to environmental gradients, Deep-Sea Res. Pt. I, 53, 1073–1099, 2006.

Bohaty, S. M., Zachos, J. C., and Delaney, M. L.: Foraminiferal Mg/Ca evidence for Southern Ocean cooling across the Eocene/Oligocene transition, Earth Planet. Sc. Lett., 317, 251–261, 2012.

Bollmann, J., Brabec, B., Cortes, M., and Geisen, M.: Determination of absolute coccolith abundances in deep-sea sediments by spiking with microbeads and spraying (SMS method), Mar. Micropaleontol., 38, 29–38, 1999.

Bordiga, M., Beaufort, L., Cobianchi, M., Lupi, C., Mancin, N., Luciani, V., Pelosi, N., and Sprovieri, M.: Calcareous plankton and geochemistry from the ODP site 1209B in the NW Pacific Ocean (Shatsky Rise): new data to interpret calcite dissolution and paleoproductivity changes of the last 450 ka, Palaeogeogr. Palaeocl., 371, 93–108, 2013.

Boscolo-Galazzo, F., Thomas, E., and Giusberti, L.: Benthic foraminiferal response to the Middle Eocene Climatic Optimum (MECO) in the South-Eastern Atlantic (ODP Site 1263), Palaeogeogr. Palaeocl., 417, 432–444, 2015.

Bown, P. R. and Dunkley Jones, T.: New Paleogene calcareous nannofossil taxa from coastal Tanzania: Tanzania Drilling Project Sites 11 to 14, Journal of Nannoplankton Research, 28, 17–34, 2006.

Bown, P. R. and Young, J. R.: Techniques, in: Calcareous Nannofossil Biostratigraphy, edited by: Bown, P. R., Chapman and Hall, Cambridge, 16–28, 1998.

Bremer, M. L. and Lohmann, G. P.: Evidence for primary control of the distribution of certain Atlantic Ocean benthonic foraminifera by degree of carbonate saturation, Deep-Sea Res., 29, 987–998, 1982.

Brown, R. E., Koeberl, C., Montanari, A., and Bice, D. M.: Evidence for a change in Milankovitch forcing caused by extraterrestrial events at Massignano, Italy, Eocene-Oligocene boundary GSSP, in: The Late Eocene Earth – Hothouse, Icehouse, and Impacts, edited by: Koeberl, C. and Montanari, A., Geol. S. Am. S., 452, 119–137, 2009.

Buccianti, A. and Esposito, P.: Insights into Late Quaternary calcareous nannoplankton assemblages under the theory of statistical analysis for compositional data, Palaeogeogr. Palaeocli., 202, 209–277, 2004.

Cachao, M. and Moita, M. T.: *Coccolithus pelagicus*, a productivity proxy related to moderate fronts off Western Iberia, Mar. Micropaleontol., 39, 131–155, 2000.

Coccioni, R.: The genera *Hantkenina* and *Cribrohantkenina* (foraminifera) in the Massignano section (Ancona, Italy), in: The Eocene–Oligocene boundary in the Marche-Umbria basin (Italy), edited by: Premoli Silva, I., Coccioni, R., and Montanari, A., International Subcommission on the Paleogene Stratigraphy, Eocene Oligocene Meeting, Ancona, Spec. Publ., 2, 81–96, 1988.

Coxall, H. K. and Pearson, P. N.: Taxonomy, biostratigraphy, and phylogeny of the Hantkeninidae (*Clavigerinella*, *Hantkenina*, and *Cribrohantkenina*), in: Atlas of Eocene Planktonic Foraminifera, edited by: Pearson, P. N., Olsson, R. K., Huber, B. T., Hemleben, C., and Berggren, W. A., Cushman Foundation Special Publication, 41, 216–256, 2006.

Coxall, H. K. and Pearson, P. N.: The Eocene-Oligocene transition, in: Deep-time perspectives on climate change: marrying the signal from computer models and biological proxies, edited by: Williams, M., et al., Geological Society (London), Micropalaeontological Society, 351–387, 2007.

Coxall, H. K. and Wilson, P. A.: Early Oligocene glaciation and productivity in the eastern equatorial Pacific: insights into global carbon cycling, Paleoceanography, 26, doi:10.1029/2010PA002021, 2011.

Coxall, H. K., Wilson, P. A., Pälike, H., Lear, C. H., and Backman, J.: Rapid stepwise onset of Antarctic glaciation and deeper calcite compensation in the Pacific Ocean, Nature, 433, 53–57, 2005.

Daniels, C. J., Sheward, R. M., and Poulton, A. J.: Biogeochemical implications of comparative growth rates of *Emiliania huxleyi* and *Coccolithus* species, Biogeosciences, 11, 6915–6925, doi:10.5194/bg-11-6915-2014, 2014.

De Kaenel, E. and Villa, G.: Oligocene-Miocene calcareous nannofossil biostratigraphy and paleoecology from the Iberia abyssal plain, in: Proceedings ODP, Scientific Results, College Station, TX (Ocean Drilling Program), 149, 79–145, 1996.

De Villiers, S.: Foraminiferal shell-weight evidence for sedimentary calcite dissolution above the lysocline. Deep-Sea Res. Pt. I, 52, 671-680, 2005.

DeConto, R. M. and Pollard, D.: Rapid Cenozoic glaciation of Antarctica induced by declining atmospheric CO_2, Nature, 421, 245–249, 2003.

Diester-Haass, L.: Middle Eocene to early Oligocene paleoceanography of the Antarctic Ocean (Maud Rise, ODP Leg 113, Site 689): change from low productivity to a high productivity ocean, Palaeogeogr. Palaeocl., 113, 311–334, 1995.

Diester-Haass, L. and Zachos, J. C.: The Eocene-Oligocene transition in the Equatorial Atlantic (ODP Site 325), paleoproductivity increase and positive $\delta^{13}C$ excursion, in: from greenhouse to icehouse: the marine Eocene-Oligocene transition, Prothero, D. R., Ivany, L. C., and Nesbitt, E. A., Columbia University Press, New York, 397–416, 2003.

Dockery III, D. T.: Punctuated succession of marine mollusks in the northern Gulf Coastal Plain, Palaios, 1, 582–589, 1986.

Dunkley Jones, T., Bown, P. R., Pearson, P. N., Wade, B. S., Coxall, H. K., and Lear, C. H.: Major shift in calcareous phytoplankton assemblages through the Eocene-Oligocene transition of Tanzania

and their implications for low-latitude primary production, Paleoceanography, 23, PA4204, doi:10.1029/2008PA001640, 2008.

Eldrett, J. S., Greenwood, D. R., Harding, I. C., and Hubber, M.: Increased seasonality through the Eocene to Oligocene transition in northern high latitudes, Nature, 459, 969–973, 2009.

Falkowski, P. G., Katz, M. E., Knoll, A. H., Quigg, A., Raven, J. A., Schofield, O., and Tayler, F. J. R.: The evolution of modern eukaryotic plankton, Science, 305, 354–360, 2004.

Fenero, R., Thomas, E., Alegret, L., and Molina, E.: Evolucion paleoambiental del transito Eocene-Oligoceno en el sur Atlantico (Sondeo 1263) basada en foraminiferos bentonicos, Geogaceta, 49, 3–6, 2010 (in Spanish).

Geisen, M., Bollmann, J., Herrle, J. O., Mutterlose, J., and Young, J. R.: Calibration of the random settling technique for calculation of absolute abundances of calcareous nannoplankton, Micropaleontology, 45, 437–442, 1999.

Gibbs, S. J., Shackleton, N. J., and Young, J. R.: Identification of dissolution patterns in nannofossil assemblages: a high-resolution comparison of synchronous records from Ceara Rise, ODP Leg 154, Paleoceanography, 19, PA1029, doi:10.1029/2003PA000958, 2004.

Gibbs, S. J., Young, J. R., Bralower, T. J., and Shackleton, N. J.: Nannofossil evolutionary events in the mid-Pliocene: an assessment of the degree of synchrony in the extinctions of *Reticulofenestra pseudoumbilicus* and *Sphenolithus abies*, Palaeogeogr. Palaeocl., 217, 155–172, 2005.

Giordano, M., Beardall, J., and Raven, A.: CO_2 concentrating mechanisms in algae: mechanisms, environmental modulation, and evolution, Annu. Rev. Plant. Biol., 56, 99–131, 2005.

Goldner, A., Herold, N., and Huber, M.: Antarctic glaciation caused ocean circulation changes at the Eocene–Oligocene transition, Nature, 511, 574–578, 2014.

Gooday, A. J.: Benthic foraminifera (Protista) as tools in deep-water palaeoceanography: environmental influences on faunal characteristics, Adv. Mar. Biol., 46, 1–90, 2003.

Gooday, A. J. and Jorisssen, F. J.: Benthic foraminiferal biogeography: controls on global distribution patterns in deep-water settings, Annual Reviews of Marine Science, 4, 237–262, 2012.

Gradstein, F. M., Ogg, J. G., Schmitz, M., and Ogg, G.: The Geologic Time Scale 2012, Vol. 2, Elsevier, 1144 pp., 2012.

Griffith, E., Calhoun, M., Thomas, E., Averyt, K., Erhardt, A., Bralower, T., Lyle, M., Olivarez-Lyle, A., and Paytan, A.: Export productivity and carbonate accumulation in the Pacific Basin at the transition from greenhouse to icehouse climate (Late Eocene to Early Oligocene), Paleoceanography, 25: PA3212, doi:10.1029/2010PA001932, 2010.

Hammer, Ø. and Harper, D. A. T.: Paleontological data analysis, Blackwell, Malden, USA, 2006.

Hammer, Ø., Harper, D. A. T., and Ryan, P. D.: PAST: Paleontological Statistics Software Package for education and data analysis, Palaeontologia Electronica, 4, 1–9, http://palaeo-electronica.org/2001_2001/past/issue2001_2001.htm, 2001.

Hannisdal, B., Henderiks, J., and Liow, L. H.: Long-term evolutionary and ecological responses of calcifying phytoplankton to changes in atmospheric CO_2, Glob. Change Biol., 18, 3504–3516, 2012.

Haq, B. U. and Lohmann, G. P.: Early Cenozoic calcareous nannoplankton biogeography of the Atlantic Ocean, Mar. Micropaleontol., 1, 119–194, 1976.

Hayek, L.-A. C. and Buzas, M. A.: Surveying natural populations: quantitative tools for assessing biodiversity, Columbia University Press, 590 pp., 2010.

Hayward, B. W., Kawagata, S., Sabaa, A. T., Grenfell, H. R., van Kerckhoven, L., Johnson, K., and Thomas, E.: The last global extinction (Mid-Pleistocene) of deep-sea benthic foraminifera (Chrysalogoniidae, Ellipsoidinidae, Glandulonodosariidae, Plectofrondiculariidae, Pleurostomellidae, Stilostomellidae), their Late Cretaceous-Cenozoic history and taxonomy. Cushman Foundation For Foraminiferal Research, Spec. Publ., 43, 408 pp., 2012.

Henderiks, J.: Coccolithophore size rules - reconstructing ancient cell geometry and cellular calcite quota from fossil coccoliths, Mar. Micropaleontol., 67, 143–154, 2008.

Henderiks, J. and Pagani, M.: Refining ancient carbon dioxide estimates: significance of coccolithophore cell size for alkenone-based pCO_2 records, Paleoceanography, 22, PA3202, doi:10.1029/2006PA001399, 2007.

Henderiks, J. and Pagani, M.: Coccolithophore cell size and Paleogene decline in atmospheric CO_2, Earth Planet. Sc. Lett., 269, 576–584, 2008.

Henderiks, J., Winter, A., Elbrächter, M., Feistel, R., van der Plas, A. K., Nausch, G., and Barlow, R.: Environmental controls on *Emiliania huxleyi* morphotypes in the Benguela coastal upwelling system (SE Atlantic), Mar. Ecol. Prog. Ser., 448, 51–66, 2012.

Hyland, E., Murphy, B., Varela, P., Marks, K., Colwell, L., Tori, F., Monechi, S., Cleaveland, L., Brinkhuis, H., Van Mourik, C. A., Coccioni, R., Bice, D., and Montanari, A.: Integrated stratigraphic and astrochronologic calibration of the Eocene-Oligocene transition in the Monte Cagnero section (northeastern Apennines, Italy): a potential parastratotype for the Massignano global stratotype section and point (GSSP), in: The Late Eocene Earth: Hothouse, Icehouse, and Impacts, edited by: Koeberl, C. and Montanari, A., Geol. S. Am. S., 452, 303–322, 2009.

Jorissen, F. J., de Stigter, H. C., and Widmark, J. G. V.: A conceptual model explaining benthic foraminiferal microhabitats, Mar. Micropaleontol., 26, 3–15, 1995.

Jorissen, F. J., Fontanier, C., and Thomas, E.: Paleoceanographical proxies based on deep-sea benthic foraminiferal assemblage characteristics, in: Proxies in Late Cenozoic Paleoceanography: Pt. 2: Biological tracers and biomarkers, edited by: Hillaire-Marcel, C. and de Vernal, A., Elsevier, 263–326, 2007.

Katz, M. E., Miller, K. G., Wright, J. D., Wade, B. S., Browning, J. V., Cramer, B. S., and Rosenthal, Y.: Stepwise transition from the Eocene greenhouse to the Oligocene icehouse, Nat. Geosci., 1, 329–334, 2008.

Keller, G: Stepwise mass extinctions and impact events: Late Eocene to early Oligocene, Mar. Micropaleontol., 10, 267–293, 1986.

Kennett, J. P.: Cenozoic evolution of Antarctic glaciation, the circum-Antarctic Ocean, and their impact on global paleoceanography, J. Geophys. Res., 82, 3843–3860, 1977.

Koch, C. and Young, J. R.: A simple weighing and dilution technique for determining absolute abundances of coccoliths from sediment samples, Journal of Nannoplankton Research, 29, 67–69, 2007.

Kucera, M. and Malmgren, B. A.: Logratio transformation of compositional data – a resolution of the constant sum constraint, Mar. Micropaleontol., 34, 117–120, 1998.

Lazarus, D. B.: The deep-sea microfossil record of macroevolutionary change in plankton and its study, in: Comparing geological and fossil records: implications for biodiversity studies, edited by: McGowan, A. J. and Smith, A. B., Geol. Soc., London, Spec. Publ., 358, 141–166, 2011.

Lear, C. H., Bailey, T. R., Pearson, P. N., Coxall, H. K., and Rosenthal, Y.: Cooling and ice growth across the Eocene-Oligocene transition, Geology, 36, 251–254, 2008.

Liu, Z., Pagani, M., Zinniker, D., DeConto, R. M., Huber, M., Brinkhuis, H., Shah, S. R., Leckie, R. M., and Pearson, A.: Global cooling during the Eocene-Oligocene climate transition, Science, 323, 1187–1190, 2009.

Lloyd, G. T., Young, J. R., and Smith, A. B.: Comparative quality and fidelity of deep-sea and land-based nannofossil records, Geology, 40, 155–158, 2012.

Lyle, M., Wilson, P. A., Janecek, T. R., et al.: Leg 199 Summary, in: Proceedings ODP, Initial Reports, College Station, TX (Ocean Drilling Program), 199, 1–87, 2002.

MacArthur, R. H.: On the relative abundance of species, Am. Nat., 94, 25–36, 1960.

Maiorano, P., Tarantino, F., Marino, M., and De Lange, G. J.: Paleoenvironmental conditions at Core KC01B (Ionina Sea) through MIS 13-9: evidence from calcareous nannofossil assemblages, Quatern. Int., 288, 97–111, 2013.

Mancin, N., Hayward, B. H., Trattenero, I., Cobianchi, M., and Lupi, C.: Can the morphology of deep-sea benthic foraminifera reveal what caused their extinction during the mid-Pleistocene

Climate Transition?, Mar. Micopaleontol., 104, 53–70, 2013.

Marino, M. and Flores, J. A.: Middle Eocene to early Oligocene calcareous nannofossil stratigraphy at Leg 177 Site 1090, Mar. Micropaleontol., 45, 291–307, 2002.

Maronna, R., Martin, R. D., and Yohai, V. J.: Robust statistics: Theory and methods, Wiley J., New York, 2006.

Martini, E.: Standard Tertiary and Quaternary calcareous nannoplankton zonation, Proc. 2nd Conf. Planktonic Microfossils, Rome, 2, 739–786, 1971.

Meng, J. and McKenna, M. C.: Faunal turnovers of Palaeogene mammals from the Mongolian Plateau, Nature, 394, 364–367, 1998.

Miller, K. G., Wright, J., and Fairbanks, R.: Unlocking the icehouse: Oligocene-Miocene oxygen isotopes, eustasy and margin erosion, J. Geophys. Res., 96, 6829–6848, 1991.

Milliman, J. D., Troy, P. J., Balch, W. M., Adams, A. K., Li, Y.-H., and Mackenzie, F. T.: Biologically mediated dissolution of calcium carbonate above the chemical lysocline? Deep-Sea Res. Pt. I, 46, 1653–1669, 1999.

Mix, A. C., Morey, A. E., Pisias, N. G., and Hostetler, S. W.: Foraminiferal faunal estimates of paleotemperature: circumventing the no-analog problem yields cool ice age tropics, Paleoceanography, 14, 350–359, doi:10.1029/1999PA900012, 1999.

Monechi, S., Buccianti, A., and Gardin, S.: Biotic signals from nannoflora across the iridium anomaly in the upper Eocene of the Massignano section: evidence from statistical analysis, Mar. Micropaleontol., 39, 219–237, 2000.

Moore, T. C., Rabinowitz, P. D., et al.: Site 525-529, in: Deep Sea Drilling Project, Initial Reports, US Government Printing Office, Washington, DC, USA, 74, 41–465, 1984.

Moore, T. C., Wade, B. S., Westerhold, T., Erhardt, A., M., Coxall, H. K., Baldauf, J., and Wagner, M.: Equatorial Pacific productivity changes near the Eocene-Oligocene boundary, Paleoceanography, 29, 825–844, doi:10.1002/2014PA002656, 2014.

Ocean Drilling Stratigraphic Network, Plate Tectonic Reconstruction Service: http://www.odsn.de/odsn/services/paleomap/paleomap.html, last access: 10 April 2015, 2011.

Okada, H. and Bukry, D.: Supplementary modification and introduction of code numbers to the low-latitude coccolith biostratigraphic zonation (Bukry, 1973; 1975), Mar. Micropaleontol., 5, 321–325, 1980.

Ortiz, S. and Thomas, E.: Deep-sea benthic foraminiferal turnover during the early middle Eocene transition at Walvis Ridge (SE Atlantic), Palaeogeogr. Palaeocl., 417, 126–136, 2015.

Pagani, M., Huber, M., Liu, Z., Bohaty, S. M., Henderiks, J., Sijp, W., Krishnan, S., and DeConto, R. M.: The role of carbon dioxide during the onset of Antarctic glaciation, Science, 334, 1261–1264, 2011.

Pälike, H., Norris, R. D., Herrle, J. O., Wilson, P. A., Coxall, H. K., Lear, C. H., Shackleton, N. J., Tripati, A. K., and Wade, B. S.: The heartbeat of the Oligocene climate system, Science, 314, 1894–1898, 2006.

Pea, L.: Eocene-Oligocene paleoceanography of the subantarctic South Atlantic: calcareous nannofossil reconstructions of temperature, nutrient, and dissolution history, Ph.D. thesis, Department of Earth Sciences, University of Parma, Italy, 210 pp., 2010.

Pearson, K.: Mathematical contributions to the theory of evolution. On a form of spurious correlation which may arise when indices are used in the measurement of organisms, P. R. Soc. London, 60, 489–498, 1896.

Pearson, P. N., van Dogen, B. E., Nicholas, C. J., Pancost, R. D., Schouten, S., Singano, J. M., and Wade, B. S.: Stable warm tropical climate through the Eocene Epoch, Geology, 35, 211–214, 2007.

Pearson, P. N., McMillan, I. K., Wade, B. S., Dunkley Jones, T., Coxall, H. K., Bown, P. R., and Lear, C. H.: Extinction and environmental change across the Eocene-Oligocene boundary in Tanzania, Geology, 36, 179–182, 2008.

Pearson, P. N., Gavin, L. F., and Wade, B. S.: Atmospheric carbon dioxide through the Eocene–Oligocene climate transition, Nature, 461, 1110–1114, 2009.

Peck, V. L., Yu, J., Kender, S., and Riesselman, C. R.: Shifting ocean carbonate chemistry during the Eocene-Oligocene climate transition: implications for deep-ocean Mg/Ca paleothermometry, Paleoceanography, 25, doi:10.1029/2009PA001906, 2010.

Persico, D. and Villa, G.: Eocene-Oligocene calcareous nannofossils from Maud Rise and Kerguelen Plateau (Antarctica): paleoecological and paleoceanographic implications, Mar. Micropaleontol., 52, 153–179, 2004.

Peterson, L. C. and Prell, W. L.: Carbonate dissolution in recent sediments of the eastern equatorial Indian Ocean: preservation patterns and carbonate loss above the lysocline, Mar. Geol., 64, 259–290, 1985.

Plancq, J., Grossi, V., Henderiks, J., Simon, L., and Mattioli, E.: Alkenone producers during late Oligocene–early Miocene revisited, Paleoceanography, 27, PA1202, doi:10.1029/2011PA002164, 2012.

Premoli Silva, I. and Jenkins, D. G.: Decision on the Eocene-Oligocene boundary stratotype, Episodes, 16, 379–382, 1993.

Raffi, I., Backman, J., Fornaciari, E., Pälike, H., Rio, D., Lourens, L., and Hilgen, F.: A review of calcareous nannofossil astrobiochronology encompassing the past 25 million years, Quaternary Sci. Rev., 25, 3113–3137, 2006.

Riesselman, C. R., Dunbar, R. B., Mucciarone, D. A., and Kitasei, S. S.: High resolution stable isotope and carbonate variability during the early Oligocene climate transition: Walvis Ridge (ODP Site 1263), in: Antarctica: A Keystone in a Changing World-Online Proceedings of the 10th ISAES, edited by: Cooper, A. K., Raymond, C. R., et al., US Geol. Surv., doi:10.3133/of2007-1047.srp095, 2007.

Rost, B., Riebesell, U., Burkhardt, S., and Sültemeyer, D.: Carbon acquisition of bloom-forming marine phytoplankton, Limnol. Oceanogr., 48, 55–67, 2003.

Rugenstein, M., Stocchi, P., von der Heijdt, A., Dijkstra, H., and Brinkhuis, H.: Emplacement of Antarctic ice sheet mass circumpolar ocean flow, Global Planet. Change, 118, 16–24, 2014.

Saavedra-Pellitero, M., Flores, J. A., Baumann, K.-H., and Sierro, F. J.: Coccolith distribution patterns in surface sediments of Equatorial and Southeastern Pacific Ocean, Geobios, 43, 131–149, 2010.

Salamy, K. A. and Zachos, J. C.: Latest Eocene-early Oligocene climate change and Southern Ocean fertility: inferences from sediment accumulation and stable isotope data, Palaeogeogr. Palaeocl., 145, 61–77, 1999.

Sarnthein, M. and Winn, K.: Reconstruction of low and middle latitude export productivity, 30,000 years BP to present: implication for global carbon reservoir, in: Climate-Ocean Interaction, edited by: Schlesinger, M. E., Kluwer Academic Publishers, 319–342, 1990.

Schumacher, S. and Lazarus, D.: Regional differences in pelagic productivity in the late Eocene to early Oligocene - a comparison of southern high latitudes and lower latitudes, Palaeogeogr. Palaeocl., 214, 243–263, 2004.

Sijp, W. P., von der Heydt, A. S., Dijkstra, H. A., Flögel, S., Douglas, P. J., and Bijl, P. K.: The role of ocean gateways on cooling climate on long time scales, Global Planet. Change, 119, 1–22, 2014.

Thomas, E.: Late Cretaceous through Neogene deep-sea benthic foraminifers (Maud Rise, Weddell Sea, Antarctica), in: Proceedings ODP, Scientific Results, College Station, TX (Ocean Drilling Program), 113, 571–594, 1990.

Thomas, E.: Middle Eocene - late Oligocene bathyal benthic foraminifera (Weddell Sea): faunal changes and implications for ocean circulation, in: Late Eocene-Oligocene climatic and biotic evolution, edited by: Prothero, D. R., and Berggren, W. A., Princeton University Press, 245–271, 1992.

Thomas, E.: Cenozoic mass extinctions in the deep sea: what disturbs the largest habitat on Earth?, in: Large ecosystem perturbations: causes and consequences, edited by: Monechi, S., Coccioni, R., and Rampino, M., Geol. S. Am. S., 424, 1–23, 2007.

Thomas, E. and Gooday, A. J.: Cenozoic deep-sea benthic foraminifers: tracers for changes in oceanic productivity?, Geology, 24, 355–358, 1996.

Tori, F.: Variabilità climatica e ciclicità nell'intervallo Eocene Oligocene: dati dai nannofossili calcarei, Ph.D. thesis, Department of Earth Sciences, University of Florence, Italy, 222 pp., 2008 (in Italian).

Via, R. K. and Thomas, D. J.: Evolution of Atlantic thermohaline circulation: Early Oligocene onset of deep-water production in the North Atlantic, Geology, 34, 441–444, 2006.

Villa, G., Fioroni, C., Pea, L., Bohaty, S., and Persico, D.: Middle Eocene-late Oligocene climate variability: calcareous nannofossil response at Kerguelen Plateau, Site 748, Mar. Micropaleontol., 69, 173–192, 2008.

Villa, G., Fioroni, C., Persico, D., Roberts, A. P., and Florindo, F.: Middle Eocene to Late Oligoce ne Antarctic glaciation/deglaciation and Southern Ocean productivity, Paleoceanography, 29, 223–237, doi:10.1002/2013PA002518, 2014.

Wei, W. and Wise, S. W.: Biogeographic gradients of middle Eocene–Oligocene calcareous nannoplankton in the South Atlantic Ocean, Palaeogeogr. Palaeocl., 79, 29–61, 1990.

Winter, A., Jordan, R. W., and Roth, P. H.: Biogeography of living coccolithophores in ocean waters, in: Coccolithophores, edited by: Winter, A. and Siesser, W. G., 161–177, 1994.

Young, J. R., Bown P.R., and Lees, J. A.: Nannotax3 website, International Nannoplankton Association, 21 Apr. 2014, URL: http://http://ina.tmsoc.org/Nannotax3, last access: 21 March 2015, 2014.

Zachos, J. C. and Kump, L. R.: Carbon cycle feedbacks and the initiation of Antarctic glaciation in the earliest Oligocene, Global Planet. Change, 47, 51–66, 2005.

Zachos, J. C., Quinn, T. M., and Salamy, K. A.: High-resolution (104 years) deep-sea foraminiferal stable isotope records of the Eocene-Oligocene climate transition, Palaeoceanography, 11, 251–266, doi:10.1029/96PA00571, 1996.

Zachos, J., Pagani, M., Sloan, L., Thomas, E., and Billups, K.: Trends, rhythms, and aberrations in global climate 65 Ma to present, Science, 292, 686–693, 2001.

Zachos, J. C., Kroon, D., Blum, P., et al.: Site 1263, in: Proceedings ODP, Initial Reports, College Station, TX (Ocean Drilling Program), 208, 1–87, 2004.

Zhang, J., Wang, P., Li, Q., Cheng, X., Jin, H., and Zhang, S.: Western equatorial Pacific productivity and carbonate dissolution over the last 550 kyr: foraminiferal and nannofossil evidence from ODP Hole 807A, Mar. Micropaleo., 64, 121–140, 2007.

Zhang, Y. G., Pagani, M., Liu, Z., Bohaty, S. M., and DeConto, R. M.: A 40-milion-year history of atmospheric CO_2, Philos. T. Roy. Soc. A., 371, 20130096, 2013.

Table caption

Table 1. Calcareous nannofossil and planktonic foraminifer bioevents as identified in this study (at meter composite depth, mcd), and the mcd reported by the Shipboard Scientific Party (Zachos et al., 2004). For each bioevent, the ages available in the most recent literature are given, as well as the location of the reference sites. N.A.: not available datum; *: ages not included in the sedimentation rate estimate.

Figure captions

Figure 1. Paleogeographic reconstruction at 33 Ma (modified from Ocean Drilling Stratigraphic Network, Plate Tectonic Reconstruction Service, www.odsn.de/odsn/services/paleomap/paleomap.html) showing location of ODP Site 1263 (black dot) on Walvis Ridge. The positions of the other sites (white squares) used for comparison and cited in the text are also given.

Figure 2. Eocene-Oligocene stratigraphy of Site 1263. Plotted against depth (mcd) are: benthic foraminifer stable isotope data (Riesselman et al., 2007), nannofossil marker species absolute abundances (N g^{-1}; note 10^7-10^8 change in scale among curves) for dataset A (grey line) and their relative percentages (%) for datasets A (black line) and B (black dashed), number of specimens > 3 chambers per gram of sediment and presence of spines of the planktonic foraminifer *Hantkenina alabamensis*. Note the changes in scales among curves. Calcareous nannofossil and planktonic foraminifer datums are highlighted. B: Base occurrence; T: Top occurrence; Bc: Base common occurrence.

Figure 3. Calcareous nannofossil abundance and distribution at Site 1263. $CaCO_3$ (wt%; Riesselman et al., 2007), coccolith dissolution index (%), H index, and the total absolute coccolith

abundance (N g^{-1}) and the mean standard deviation percentage on 5 samples are plotted against depth. The absolute (N g^{-1}, black solid line) and relative (%, grey dotted line) abundances of the main species which constitute the assemblage are displayed. For *Cyclicargolithus* sp. and *C. pelagicus* also the absolute abundances of the size groups are shown. The grey bar close to the dissolution index identifies an interval of major dissolution.

Figure 4. Distribution patterns of PC1 **(a)** and PC2 **(b)** obtained from the PCA for the datasets A and B (light green curves). Loadings of calcareous nannofossil taxa on the two principal components of the whole studied succession for dataset A are reported. The shaded boxes represent the most relevant loaded species. Shaded area: PCs (dataset A) obtained omitting the marker species in the dataset. Red line: PCs (dataset A) obtained inserting also the marker species.

Figure 5. Coccolith total abundance (N g^{-1}), PC1 and cell-size trends during the Eocene-Oligocene at Site 1263. The average cell V:SA (μm) of all placolith-bearing species (green area), *Reticulofenestra-Dictyococcites-Cyclicargolithus* (red solid line) and *Reticulofenestra-Dictyococcites* (green dotted line) are reported. The average cell V:SA of ODP 925 (black circles; Pagani et al., 2011), DSDP 516 (white triangles; Henderiks and Pagani, 2008), DSDP 511-277 (white squares) and ODP 1090 (black squares) from the southern ocean (Pagani et al., 2011), and pCO_2 (ppm) alkenone-based from ODP 925 (white circles; Zhang et al., 2013), ODP 929 (black circles; Pagani et al., 2011), and pCO_2 boron isotope-based from TDP12/17 (grey triangles; Pearson et al., 2009) are also shown. For comparison with sea surface temperature (SST) proxies, the Mg/Ca (mmol/mol; Peck et al., 2010) at Site 1263 and the SST from $U^{k'}_{37}$ at low latitude in the Atlantic Ocean (Liu et al., 2009) are also displayed.

Figure 6. Paleoproductivity indices from nannofossil (PC2) and benthic foraminifer ($\Delta\delta^{13}C_{P-B}$ calculated from data in Riesselman et al., 2007 and Peck et al., 2010; Fisher's alpha index - diversity proxy, extinction group species, phytodetritus using species, buliminid species and the species *Nuttalides umbonifera*) datums are plotted against depth.

Table 1

	This study		Shipboard Scientific Party (Zachos et al., 2004)	Ages		
Datum	**(hole-core-section, cm)**	**Depth (mcd)**	**Average Depth (mcd)**	**Age (Ma)**	**Site/Area**	**References**
T *Isthmolithus recurvus*	B-3H-5, 115-116	83.19	86	32.7	Leg 199	Lyle et al. (2002)
T *Coccolithus formosus*	A-9H-4, 9-10	85.16	86	32.92	Site 1218	Gradstein et al. (2012)
Bc *Sphenolithus akropodus*	A-9H-4, 100-102	86.34	N.A.			
B *Chiasmolithus altus*	B-4H-2, 131-132	89.4	N.A.	33.31*	Site 1218	Pälike et al. (2006)
B *Sphenolithus akropodus*	B-4H-3, 50-52	90.09	N.A.			
AB *Clausicoccus obrutus*	A-10H-4, 141-142	96	94.77	33.85*	Massignan GSSP	Brown et al. (2009)
T *Hantkenina* spp.	A-10H-5, 32-34	96.27	104.5	33.89	Mediterranean	Gradstein et al. (2012)
T *Discoaster saipanensis*	B-5H-3, 50-52	102.27	104.1	34.44	Site 1218	Gradstein et al. (2012)
T *Discoaster barbadiensis*	B-5H-4, 0-2	103.27	N.A.	34.76	Site 1218	Gradstein et al. (2012)
B *Sphenolithus tribulosus*	B-5H-4, 50-52	103.77	N.A.			

Fig. 1

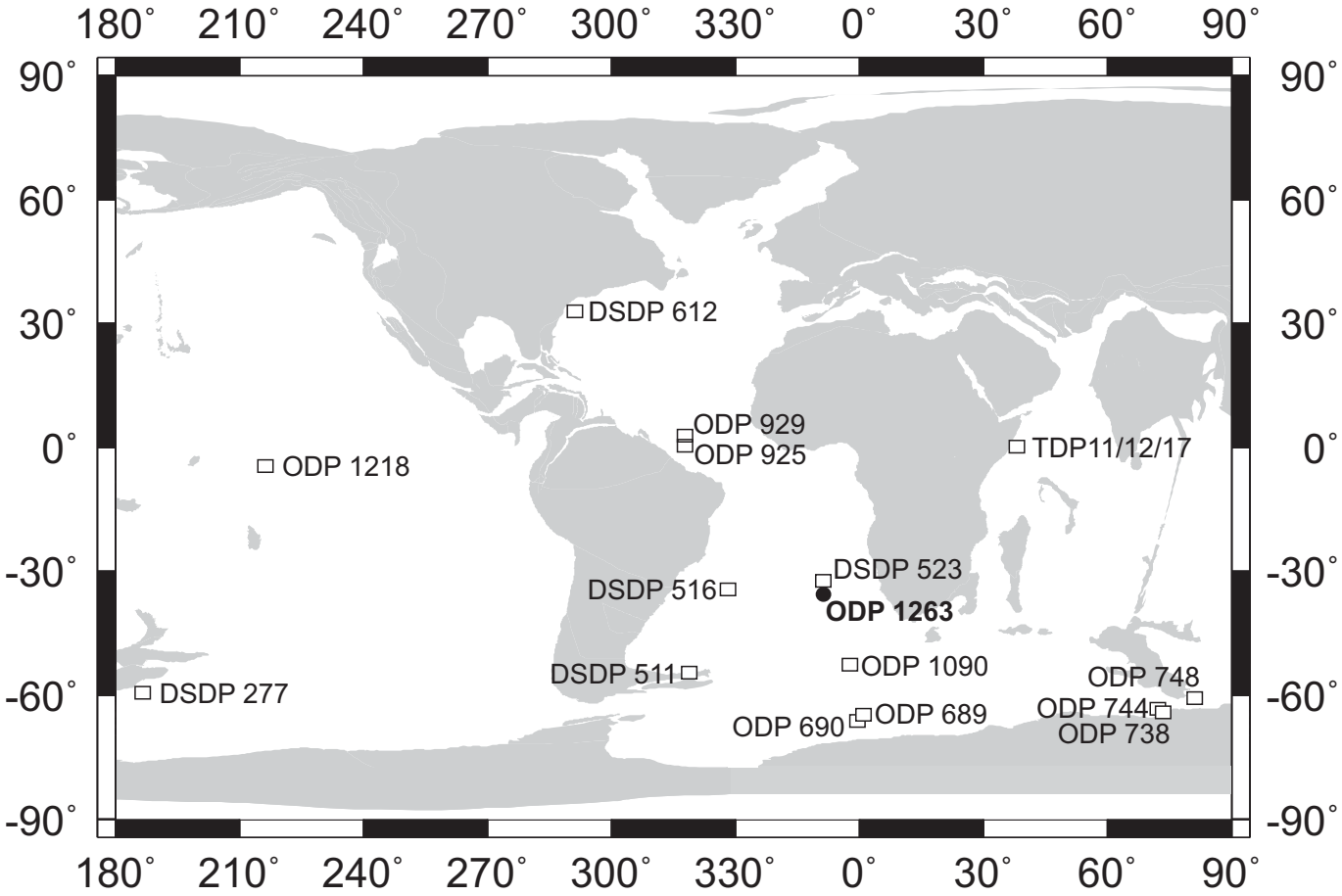
180˚ 210˚ 240˚ 270˚ 300˚ 330˚ 0˚ 30˚ 60˚ 90˚
90˚
60˚
30˚
0˚
-30˚
-60˚
-90˚
DSDP 612
ODP 929
ODP 925
ODP 1218
TDP11/12/17
DSDP 523
DSDP 516
ODP 1263
ODP 1090
DSDP 511
ODP 748
DSDP 277
ODP 744
ODP 690
ODP 689
ODP 738

Fig. 2

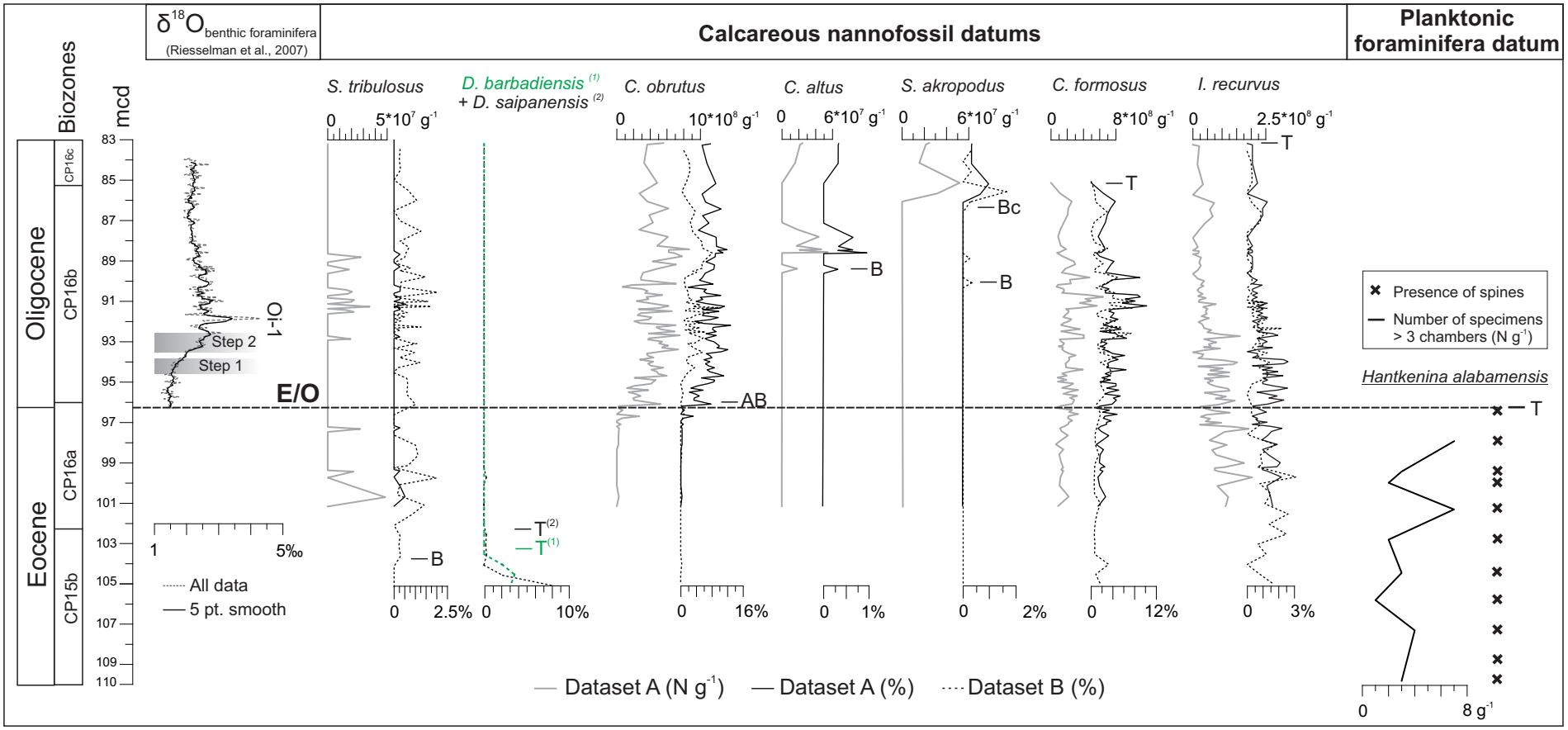
δ18O benthic foraminifera (Riesselman et al., 2007)
Calcareous nannofossil datums
Planktonic foraminifera datum
Biozones
mcd
Oligocene
Eocene
CP16c
CP16b
CP16a
CP15b
Oi-1
Step 2
Step 1
E/O
1
5‰
All data
5 pt. smooth
S. tribulosus
D. barbadiensis (1) + D. saipanensis (2)
C. obrutus
C. altus
S. akropodus
C. formosus
I. recurvus
0 5*10^7 g^-1
0 10*10^8 g^-1
0 6*10^7 g^-1
0 6*10^7 g^-1
0 8*10^8 g^-1
0 2.5*10^8 g^-1
T
Bc
B
AB
T(2)
T(1)
0 2.5%
0 10%
0 16%
0 1%
0 2%
0 12%
0 3%
Presence of spines
Number of specimens > 3 chambers (N g^-1)
Hantkenina alabamensis
0 8 g^-1
Dataset A (N g^-1)
Dataset A (%)
Dataset B (%)

Fig. 3

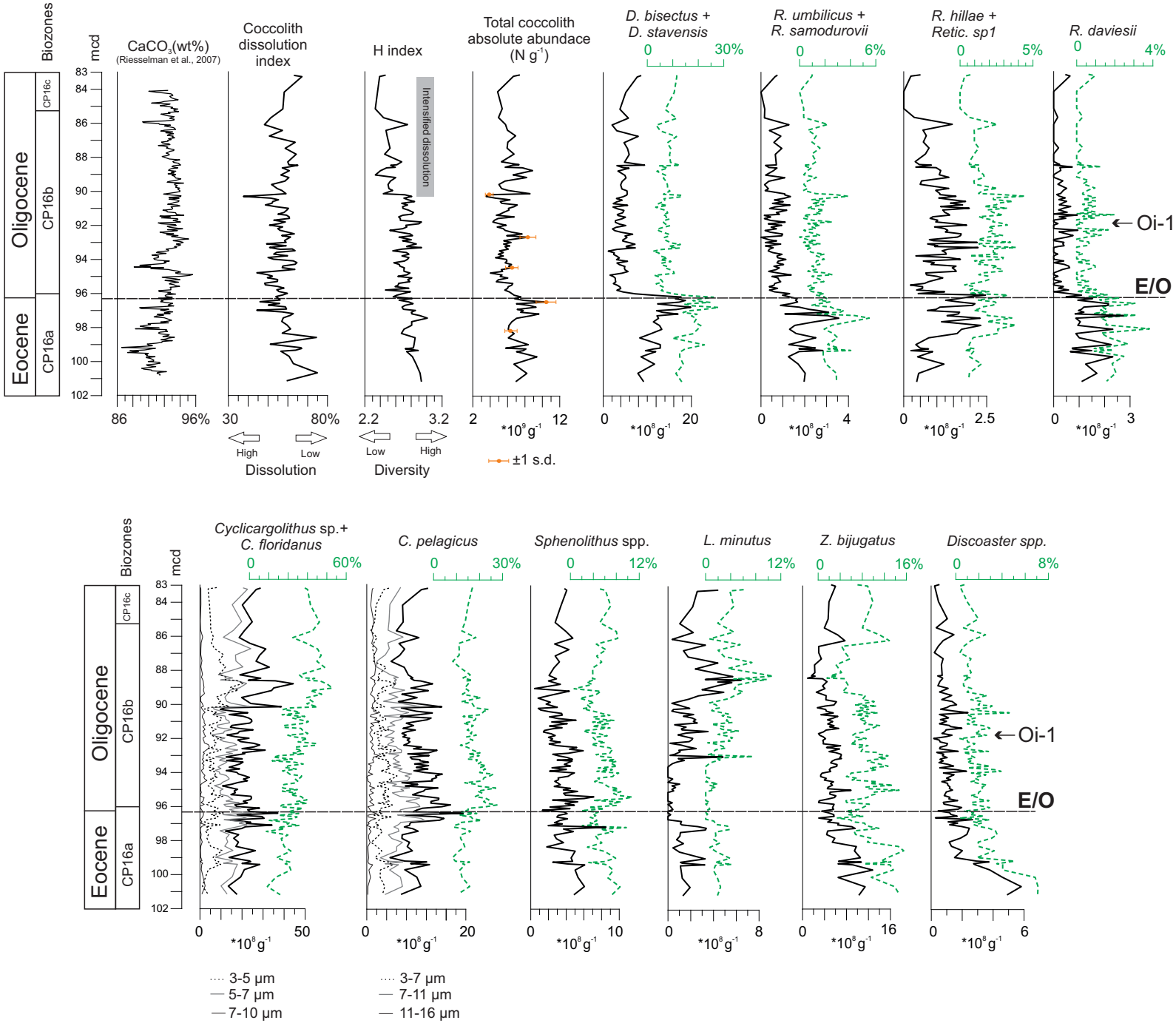
Biozones
mcd
Oligocene
Eocene
CP16c
CP16b
CP16a
CaCO3(wt%)
(Riesselman et al., 2007)
Coccolith dissolution index
H index
Intensified dissolution
Total coccolith absolute abundace (N g-1)
D. bisectus + D. stavensis
R. umbilicus + R. samodurovii
R. hillae + Retic. sp1
R. daviesii
Oi-1
E/O
High
Low
Dissolution
Diversity
±1 s.d.
Cyclicargolithus sp.+ C. floridanus
C. pelagicus
Sphenolithus spp.
L. minutus
Z. bijugatus
Discoaster spp.
3-5 µm
5-7 µm
7-10 µm
3-7 µm
7-11 µm
11-16 µm

Fig. 4

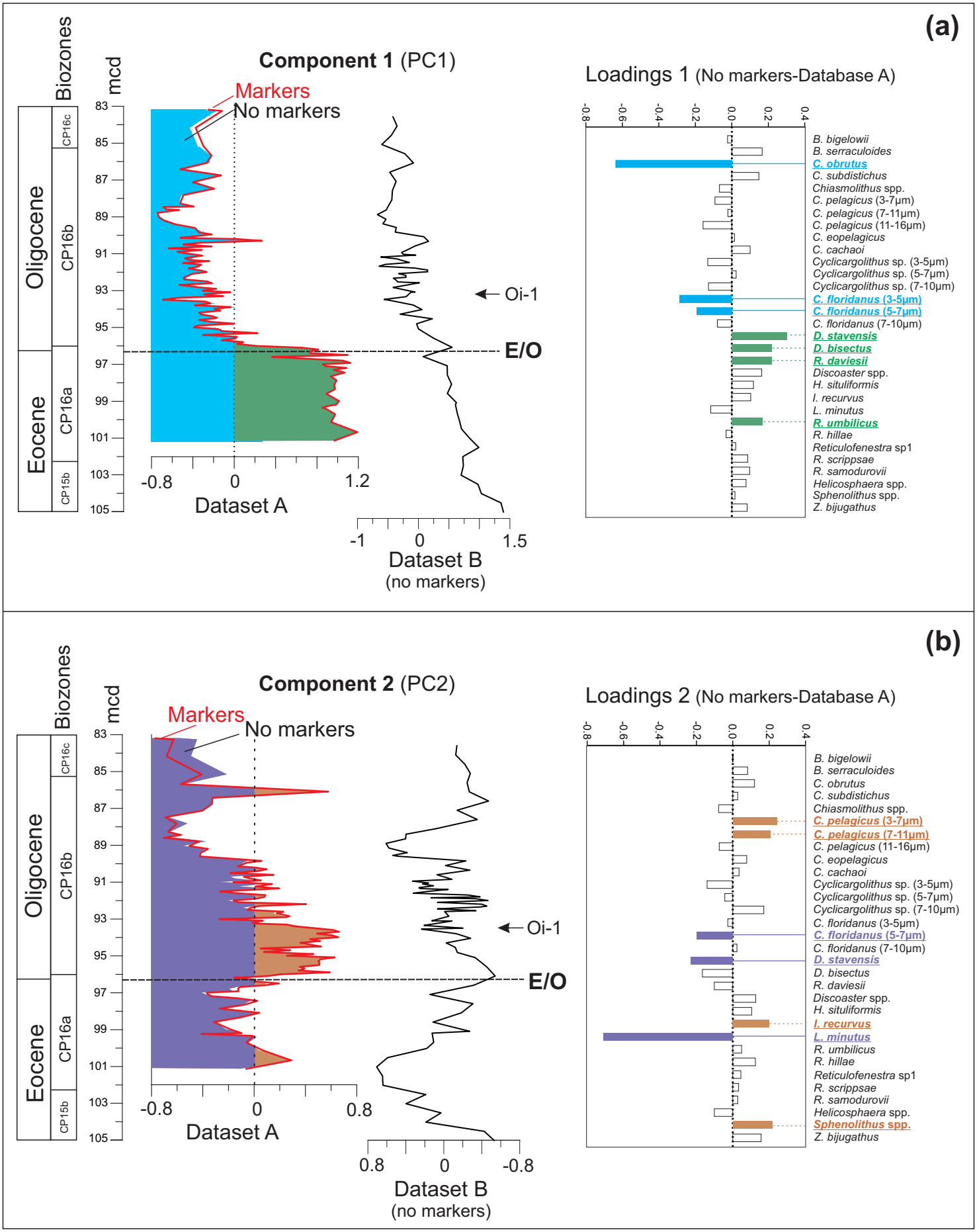
(a)
Biozones
mcd
Oligocene
Eocene
CP16c
CP16b
CP16a
CP15b
Component 1 (PC1)
Markers
No markers
Oi-1
E/O
Dataset A
Dataset B
(no markers)
Loadings 1 (No markers-Database A)
B. bigelowii
B. serraculoides
C. obrutus
C. subdistichus
Chiasmolithus spp.
C. pelagicus (3-7µm)
C. pelagicus (7-11µm)
C. pelagicus (11-16µm)
C. eopelagicus
C. cachaoi
Cyclicargolithus sp. (3-5µm)
Cyclicargolithus sp. (5-7µm)
Cyclicargolithus sp. (7-10µm)
C. floridanus (3-5µm)
C. floridanus (5-7µm)
C. floridanus (7-10µm)
D. stavensis
D. bisectus
R. daviesii
Discoaster spp.
H. situliformis
I. recurvus
L. minutus
R. umbilicus
R. hillae
Reticulofenestra sp1
R. scrippsae
R. samodurovii
Helicosphaera spp.
Sphenolithus spp.
Z. bijugathus
(b)
Component 2 (PC2)
Loadings 2 (No markers-Database A)

Fig. 5

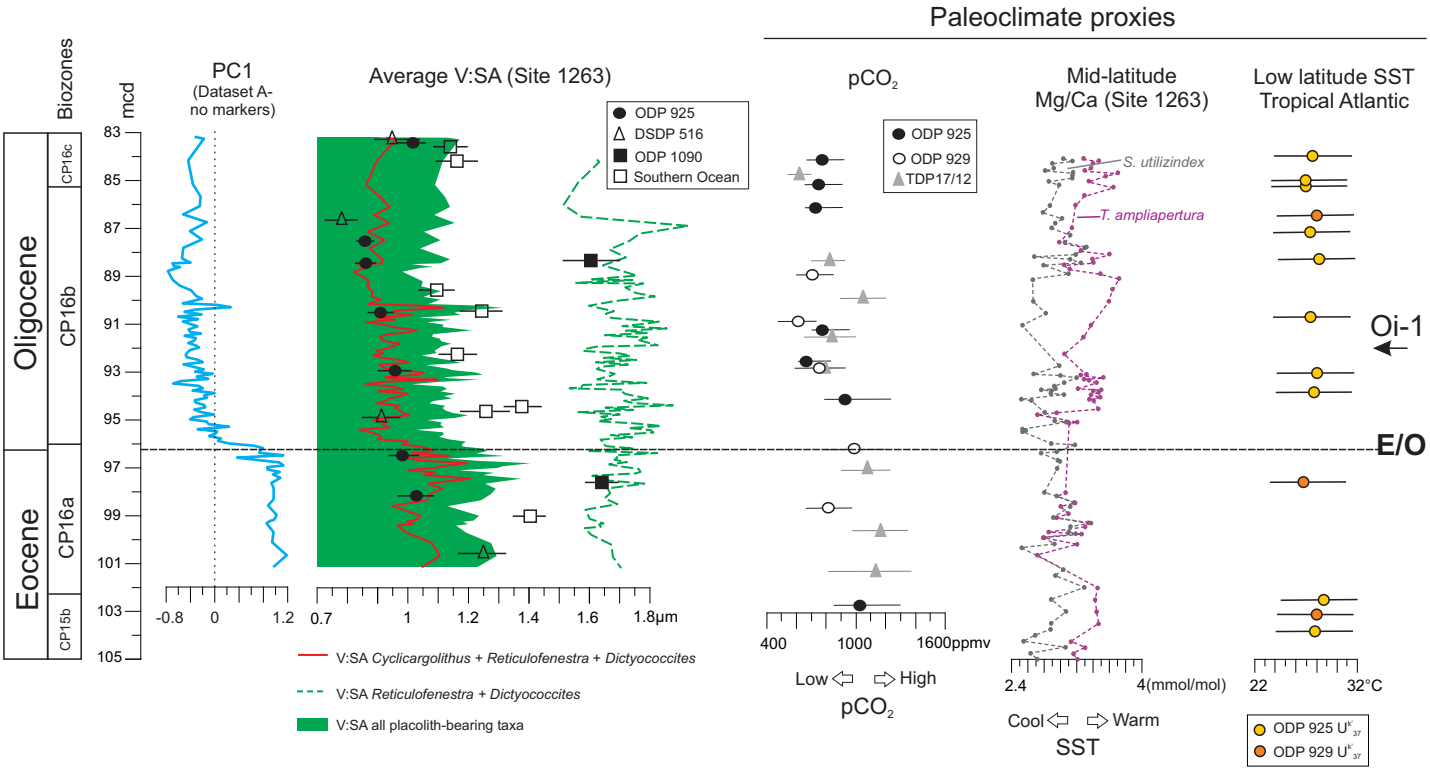
Paleoclimate proxies
Biozones
mcd
Oligocene
Eocene
CP16c
CP16b
CP16a
CP15b
PC1
(Dataset A-
no markers)
Average V:SA (Site 1263)
ODP 925
DSDP 516
ODP 1090
Southern Ocean
pCO2
ODP 925
ODP 929
TDP17/12
Mid-latitude
Mg/Ca (Site 1263)
S. utilizindex
T. ampliapertura
Low latitude SST
Tropical Atlantic
Oi-1
E/O
V:SA Cyclicargolithus + Reticulofenestra + Dictyococcites
V:SA Reticulofenestra + Dictyococcites
V:SA all placolith-bearing taxa
Low High
pCO2
Cool Warm
SST
ODP 925 U37K
ODP 929 U37K

Fig. 6

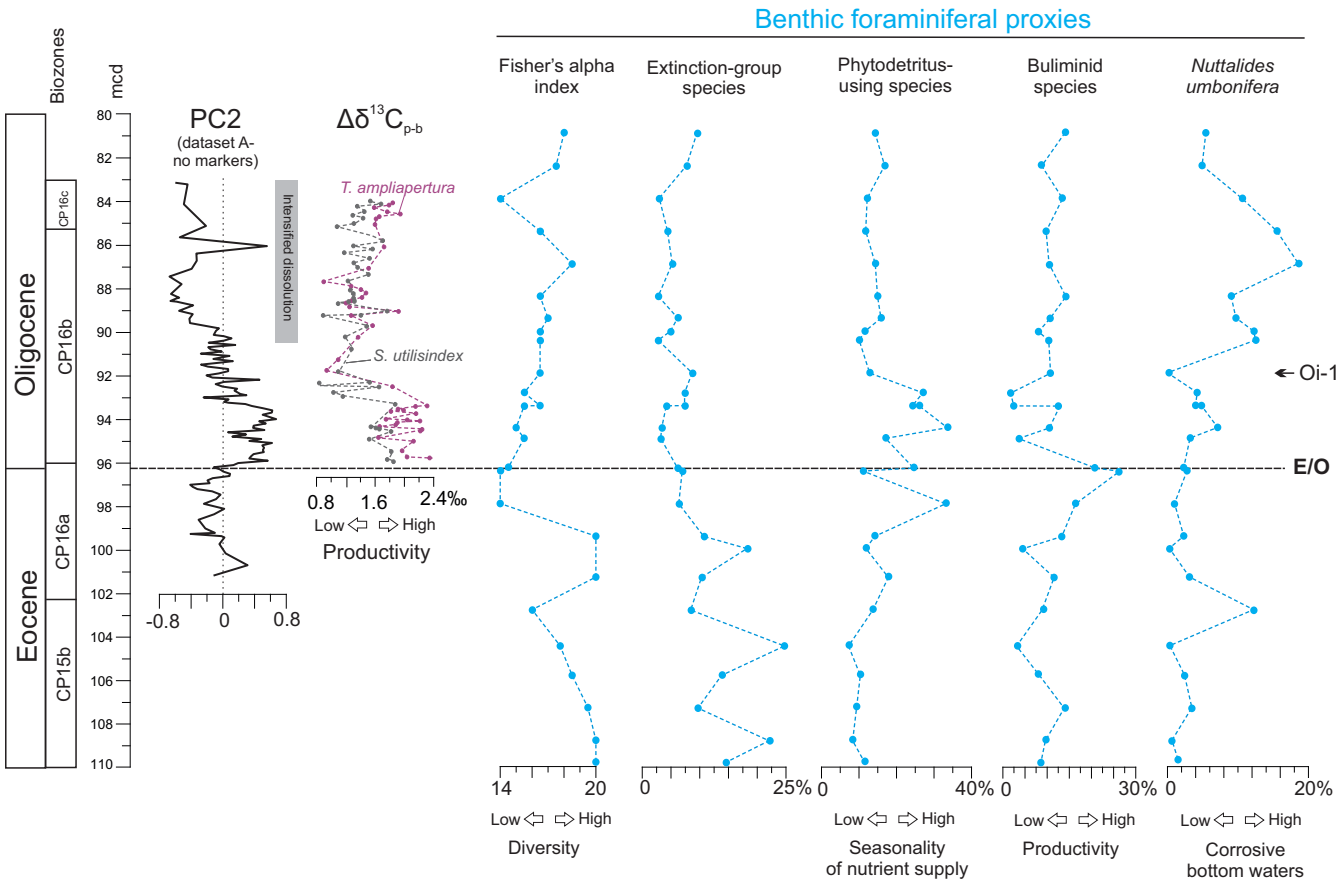
Benthic foraminiferal proxies
Biozones
mcd
Oligocene
Eocene
CP16c
CP16b
CP16a
CP15b
PC2
(dataset A-
no markers)
Intensified dissolution
Δδ13Cp-b
T. ampliapertura
S. utilisindex
0.8
1.6
2.4‰
Low High
Productivity
-0.8
0
0.8
Fisher's alpha index
Extinction-group species
Phytodetritus-using species
Buliminid species
Nuttalides umbonifera
Oi-1
E/O
14
20
Low High
Diversity
0
25%
Seasonality of nutrient supply
40%
30%
20%
Corrosive bottom waters